

Global Ocean Monitoring: Recent Evolution, Current Status, and Predictions

Prepared by
Climate Prediction Center, NCEP/NOAA
March 12, 2019

<http://www.cpc.ncep.noaa.gov/products/GODAS/>

**This project to deliver real-time ocean monitoring products is implemented
by CPC in cooperation with NOAA's Ocean Observing and Monitoring Division (OOMD)**

Outline

- **Overview**
- **Recent highlights**
 - **Pacific/Arctic Ocean**
 - **Indian Ocean**
 - **Atlantic Ocean**
 - **Global SST Predictions**
- **Challenges of Forecasting ENSO Cycle**

Overview

➤ Pacific Ocean

- ❑ NOAA “ENSO Diagnostic Discussion” on 14 Feb 2019 indicated that “*Weak El Nino conditions are present and are expected to continue through the Northern Hemisphere spring 2019 (~55% chance).*”
- ❑ Positive SSTAs persisted in the central and eastern tropical Pacific with NINO3.4=0.66°C in Feb 2019.
- ❑ Positive subsurface ocean temperature anomalies presented along the equatorial Pacific and propagated eastward in Feb 2019.
- ❑ Positive SST anomalies presented in the N. Pacific with PDOI=-0.1 in Feb 2019.

➤ Indian Ocean

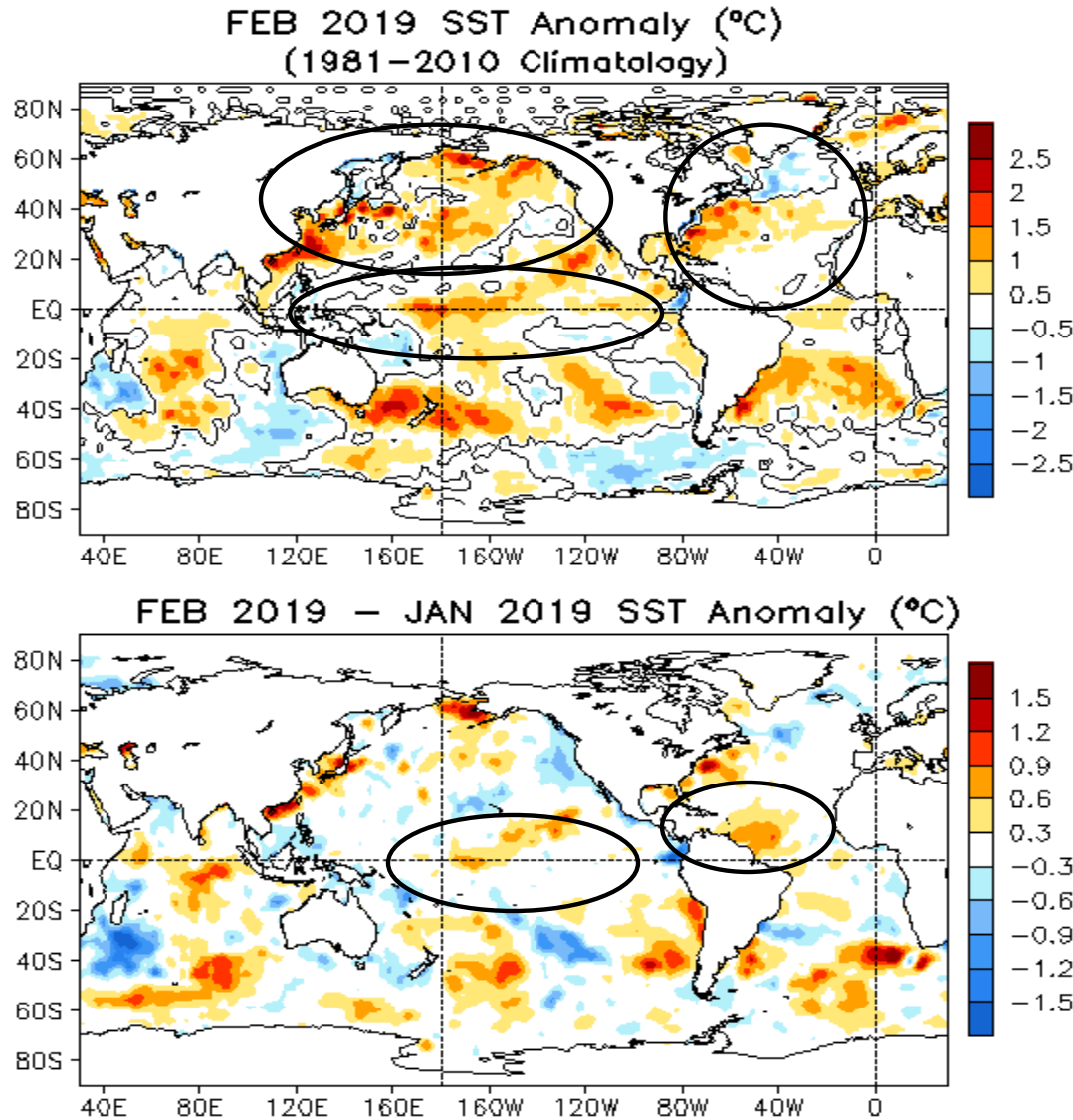
- ❑ SSTAs were near average in the tropics in Feb 2019.

➤ Atlantic Ocean

- ❑ NAO was in a neutral phase with NAOI=-0.1 in Feb 2019, and SSTAs were a tripole/horseshoe pattern with positive anomalies in the middle latitudes of N. Atlantic in the last few years.

Global Oceans

Global SST Anomaly ($^{\circ}\text{C}$) and Anomaly Tendency



- Positive SSTAs were mainly in the central tropical Pacific, consistent with El Niño conditions.

- Positive SSTAs were in the North Pacific.

- Horseshoe/tripole-like SSTA pattern presented in the North Atlantic.

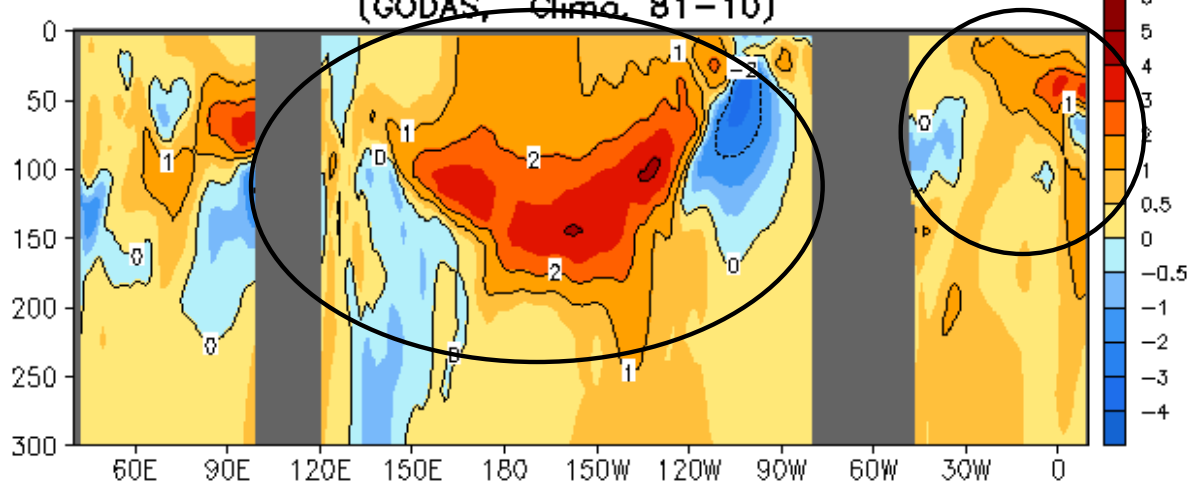
- In the Indian Ocean, SSTAs were near average in the tropics.

- Positive SSTA tendencies were observed in the central tropical Pacific, and also in the tropical Northwestern Atlantic Ocean.

Fig. G1. Sea surface temperature anomalies (top) and anomaly tendency (bottom). Data are derived from the NCEP OI SST analysis, and anomalies are departures from the 1981–2010 base period means.

Longitude-Depth Temperature Anomaly and Anomaly Tendency in 2°S-2°N

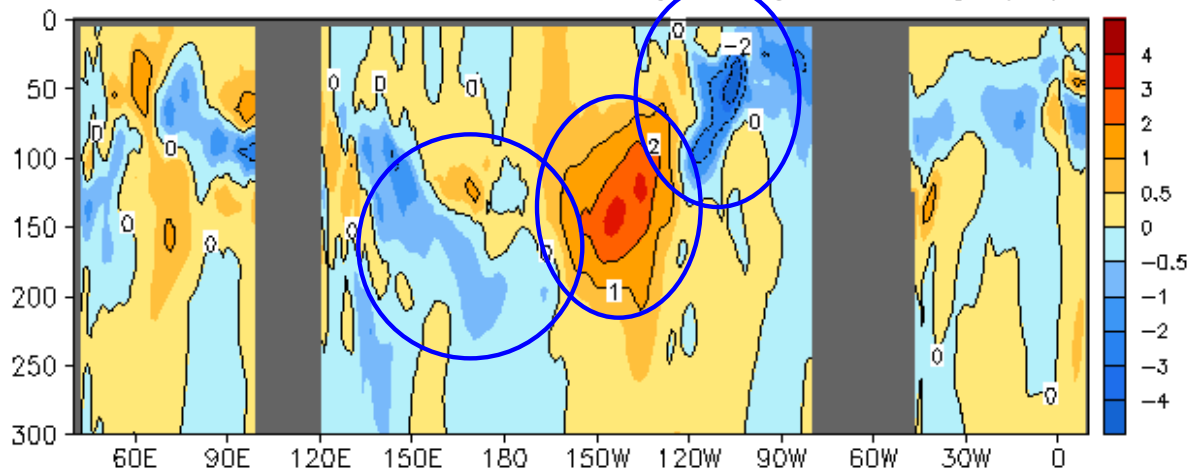
FEB 2019 Eq. Temp Anomaly (°C)
(GODAS, Climo. 81-10)



- Positive (negative) ocean temperature anomalies presented along the thermocline in the central (far eastern) Pacific.

- Positive ocean temperature anomalies were in the eastern and negative in the western Atlantic and Indian Oceans.

FEB 2019 - JAN 2019 Eq. Temp Anomaly (°C)

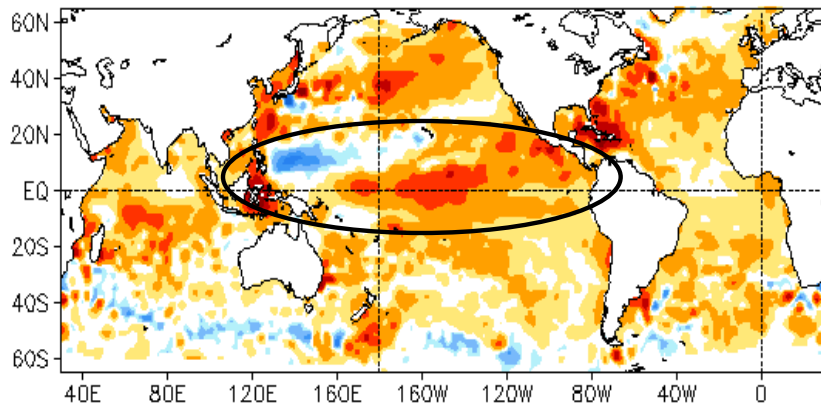


- Anomalous temperature tendency displayed a tripole pattern in the Pacific Ocean: positive in the central, and negative to the west and east.

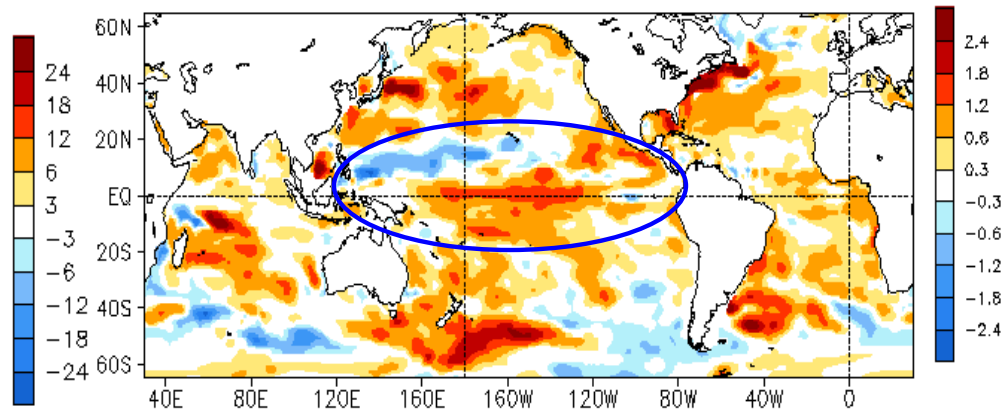
Fig. G3. Equatorial depth-longitude section of ocean temperature anomalies (top) and anomaly tendency (bottom). Data are derived from the NCEP's global ocean data assimilation system which assimilates oceanic observations into an oceanic GCM. Anomalies are departures from the 1981-2010 base period means.

Global SSH and HC300 Anomaly & Anomaly Tendency

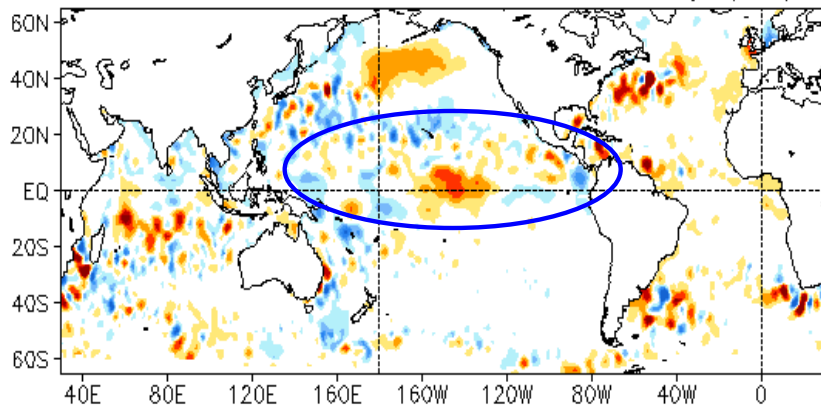
FEB 2019 SSH Anomaly (cm)
(AVISO Altimetry, Climo. 93-13)



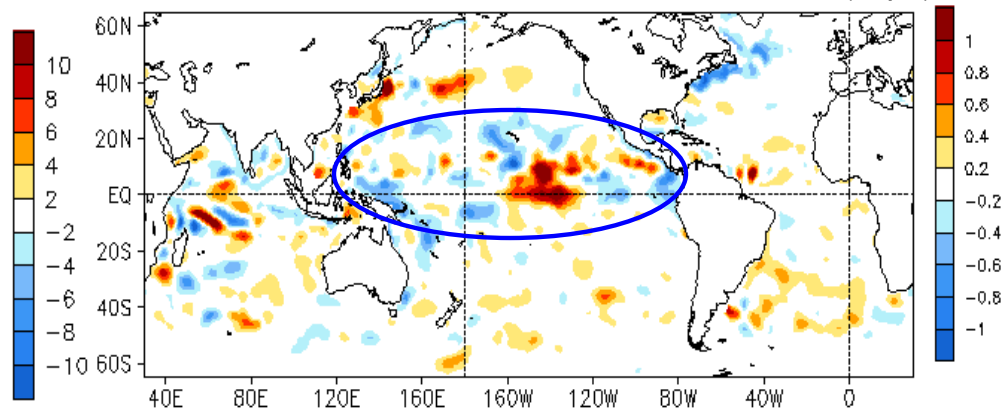
FEB 2019 Heat Content Anomaly (°C)
(GODAS, Climo. 81-10)



FEB 2019 - JAN 2019 SSH Anomaly (cm)



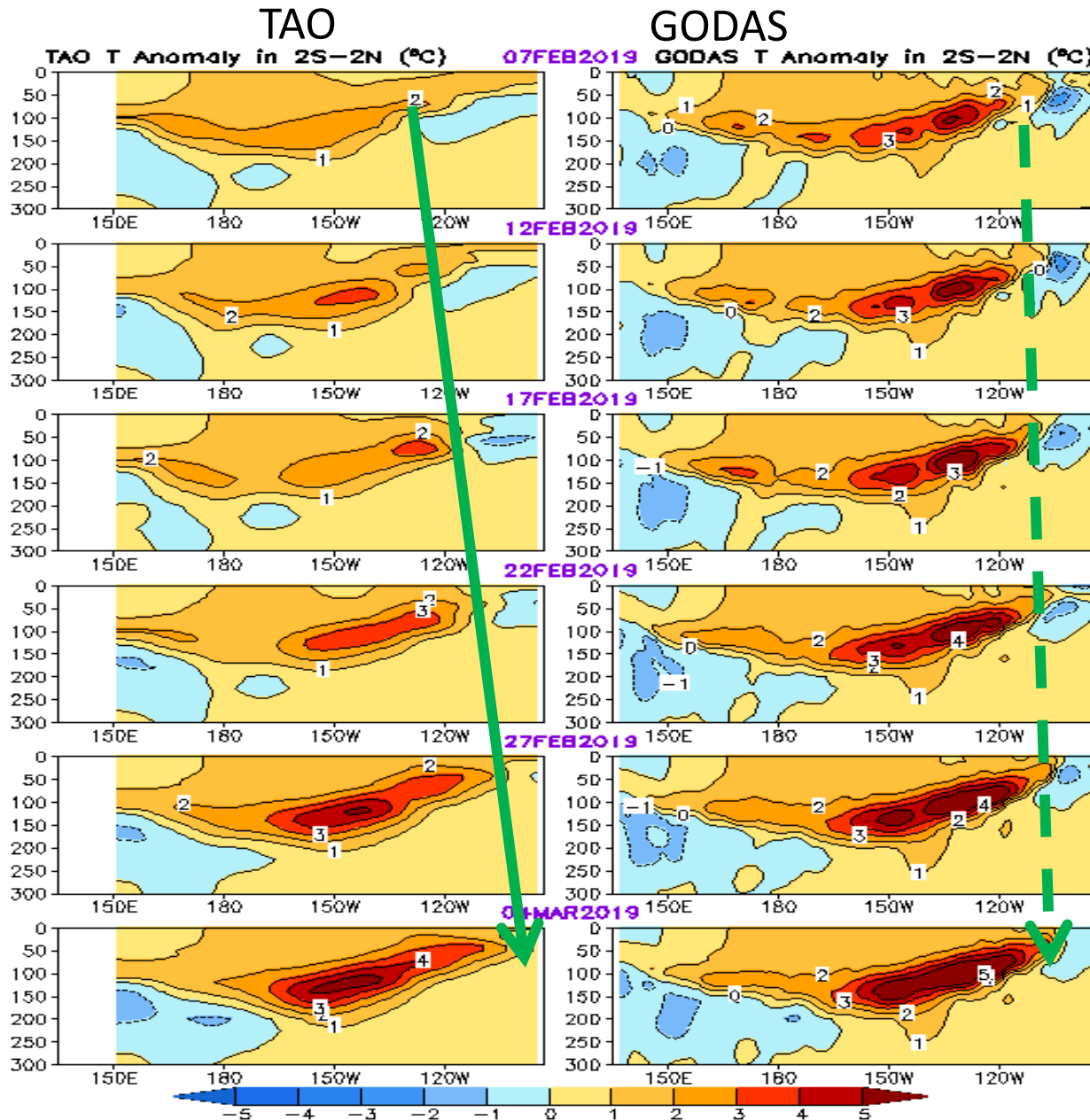
FEB 2019 - JAN 2019 Heat Content Anomaly (°C)



- The SSHA pattern was overall consistent with HC300A pattern, but there were many detailed differences between them.
- Both SSHA and HC300A in the tropical Pacific were consistent with the El Nino conditions.
- Positive tendencies of SSHA and HC300A presented in the east-central tropical Pacific.

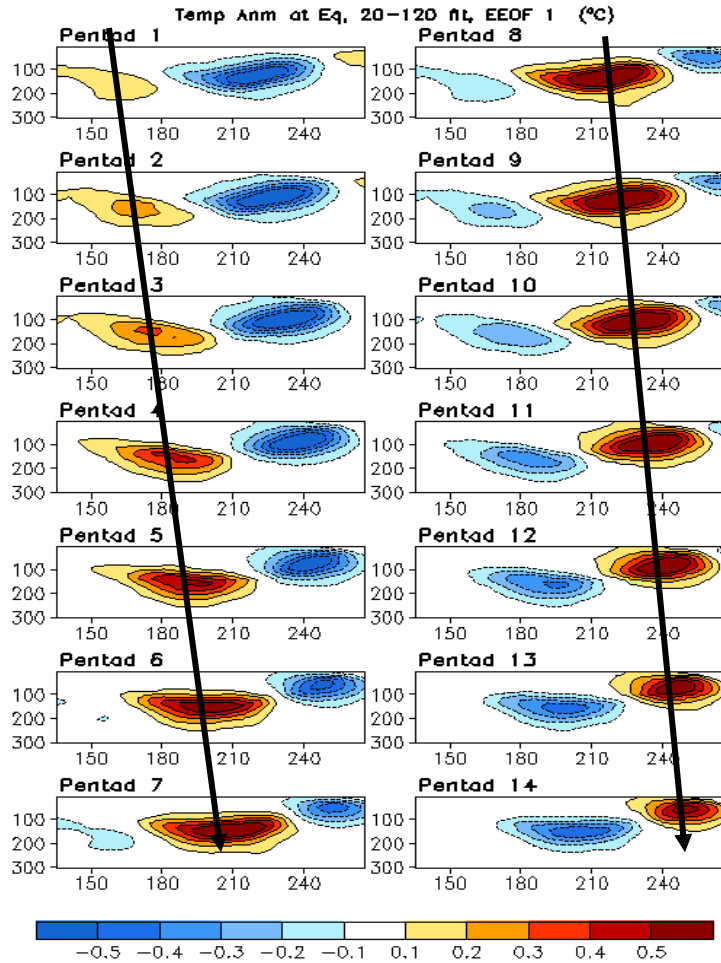
Tropical Pacific Ocean and ENSO **Conditions**

Equatorial Pacific Ocean Temperature Pentad Mean Anomaly

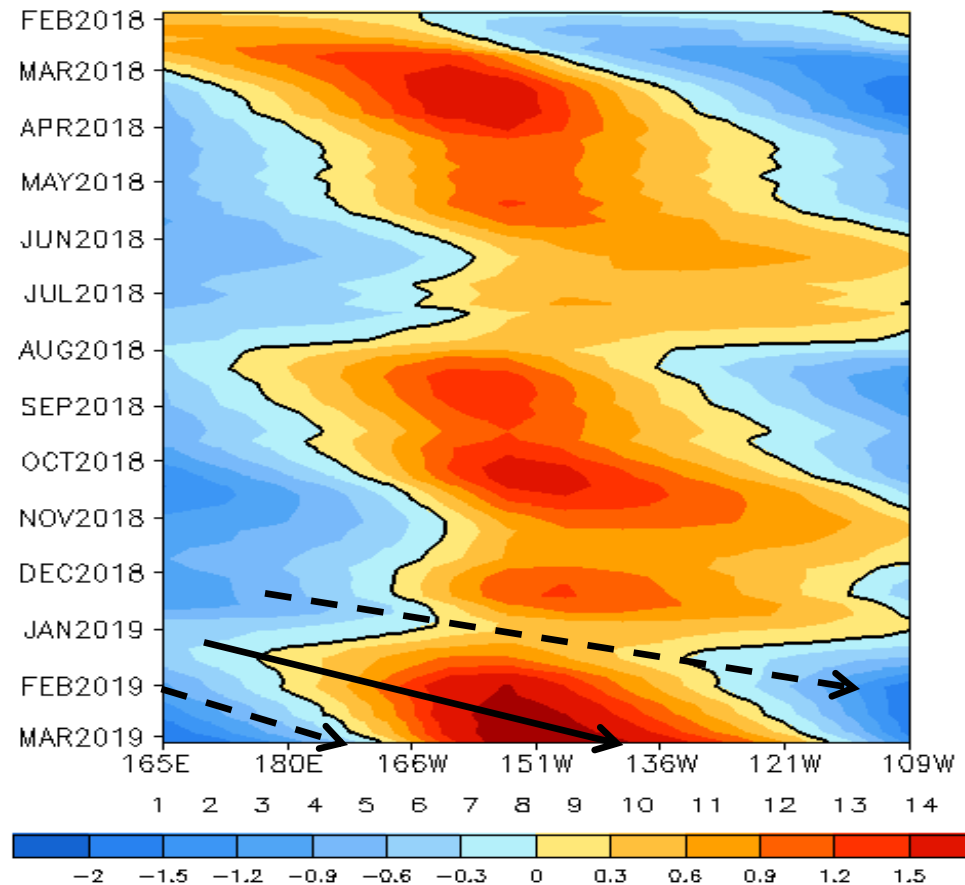


- Enhanced positive ocean temperature anomalies during the last month were associated with the downwelling Kelvin wave.
- The eastward propagation of ocean temperature anomalies was more visible in TAO than in GODAS.

Oceanic Kelvin Wave (OKW) Index



Standardized Projection on EEOF 1

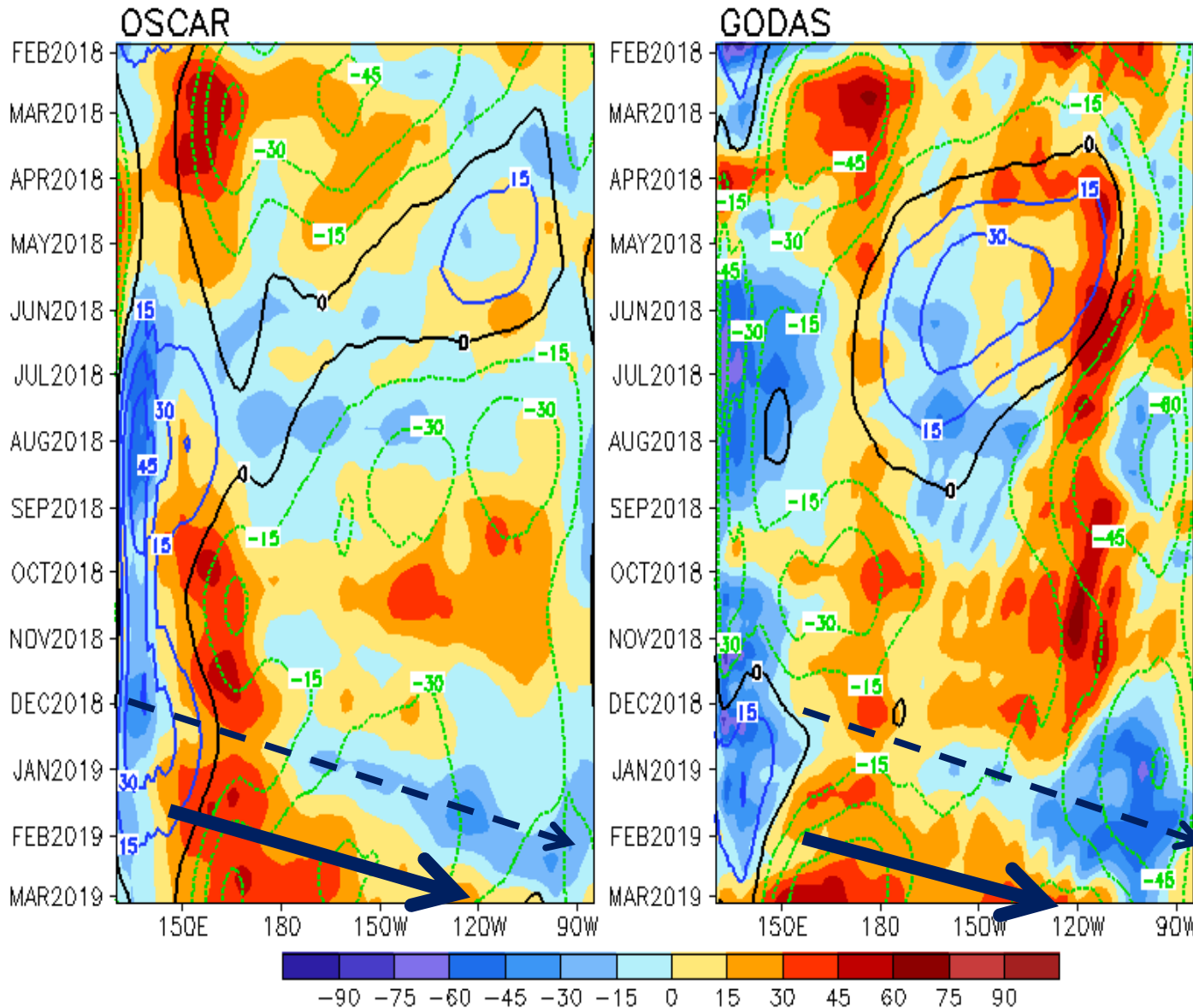


- A downwelling Kelvin wave presented from Jan- Feb 2019, leading to increasing positive subsurface anomalies in the central and eastern tropical Pacific.

(OKW index is defined as standardized projections of total anomalies onto the 14 patterns of Extended EOF1 of equatorial temperature anomalies (Seo and Xue , GRL, 2005).)

Evolution of Equatorial Pacific Surface Zonal Current Anomaly (cm/s)

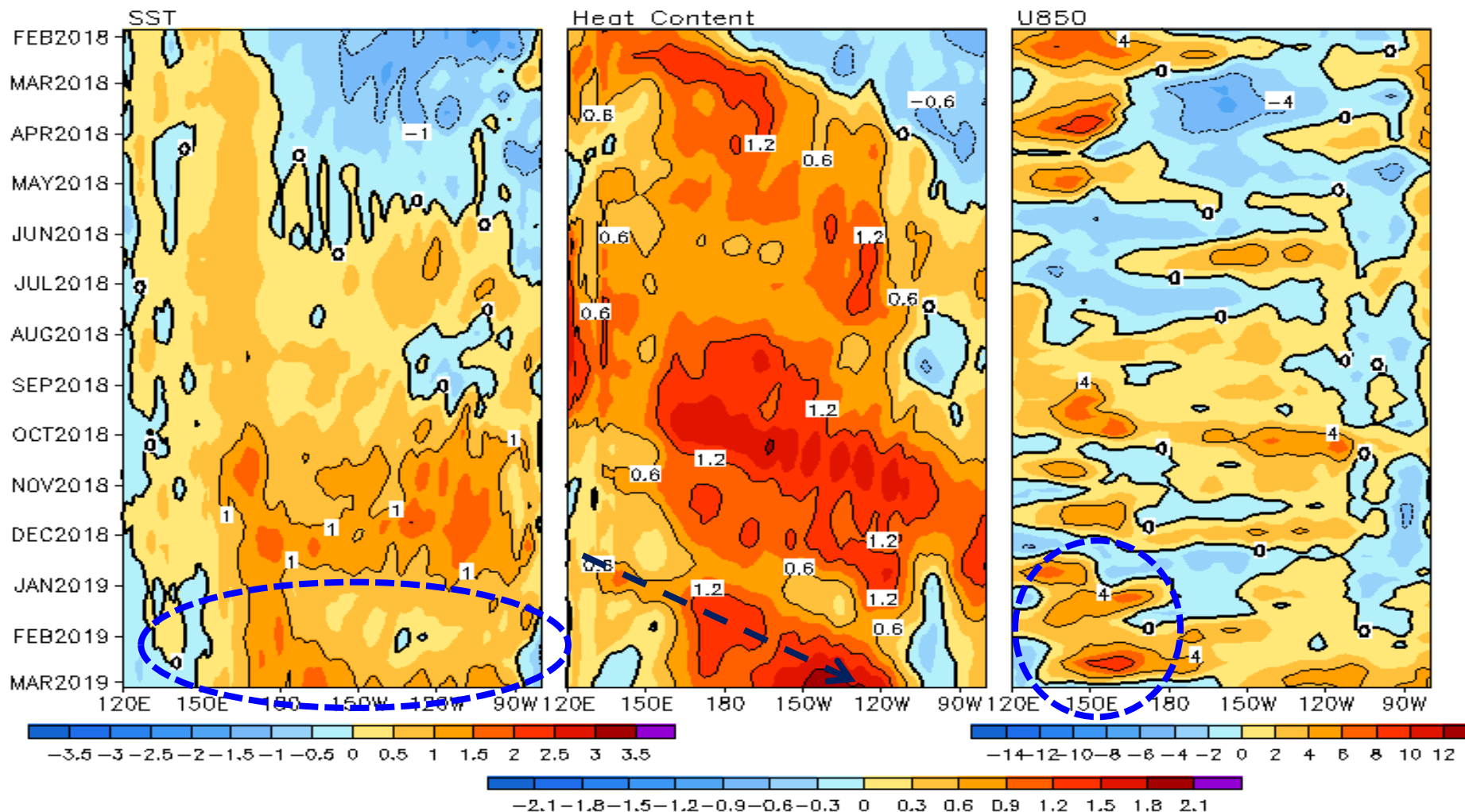
U (15m), cm/s, 2°S–2°N (Shading=Anomaly; Contour=Climatology)



- Anomalous eastward currents expanded eastward in the last two months in OSCAR and GODAS. That was favorable for increase of the positive SSTA.
- The anomalous currents showed some differences between OSCAR and GODAS.

Equatorial Pacific SST (°C), HC300 (°C), u850 (m/s) Anomalies

2°S–2°N Average, 3 Pentad Running Mean



- Positive SSTA in the central and eastern Pacific strengthened in the last month.
- Positive HC300A propagated eastward in Feb 2019, and low-level westerly wind burst was observed in Feb 2019, consistent with the Kelvin wave activity.

Warm Water Volume (WWV) and NINO3.4 Anomalies

- WWV is defined as average of depth of 20°C in [120°E-80°W, 5°S-5°N].

Statistically, peak correlation of Nino3 with WWV occurs at 7 month lag (Meinen and McPhaden, 2000).

- Since WWV is intimately linked to ENSO variability (Wyrtki 1985; Jin 1997), it is useful to monitor ENSO in a phase space of WWV and NINO3.4 (Kessler 2002).

- Increase (decrease) of WWV indicates recharge (discharge) of the equatorial oceanic heat content.

- Equatorial Warm Water Volume (WWV) indicated an overall discharging since Oct 2018.

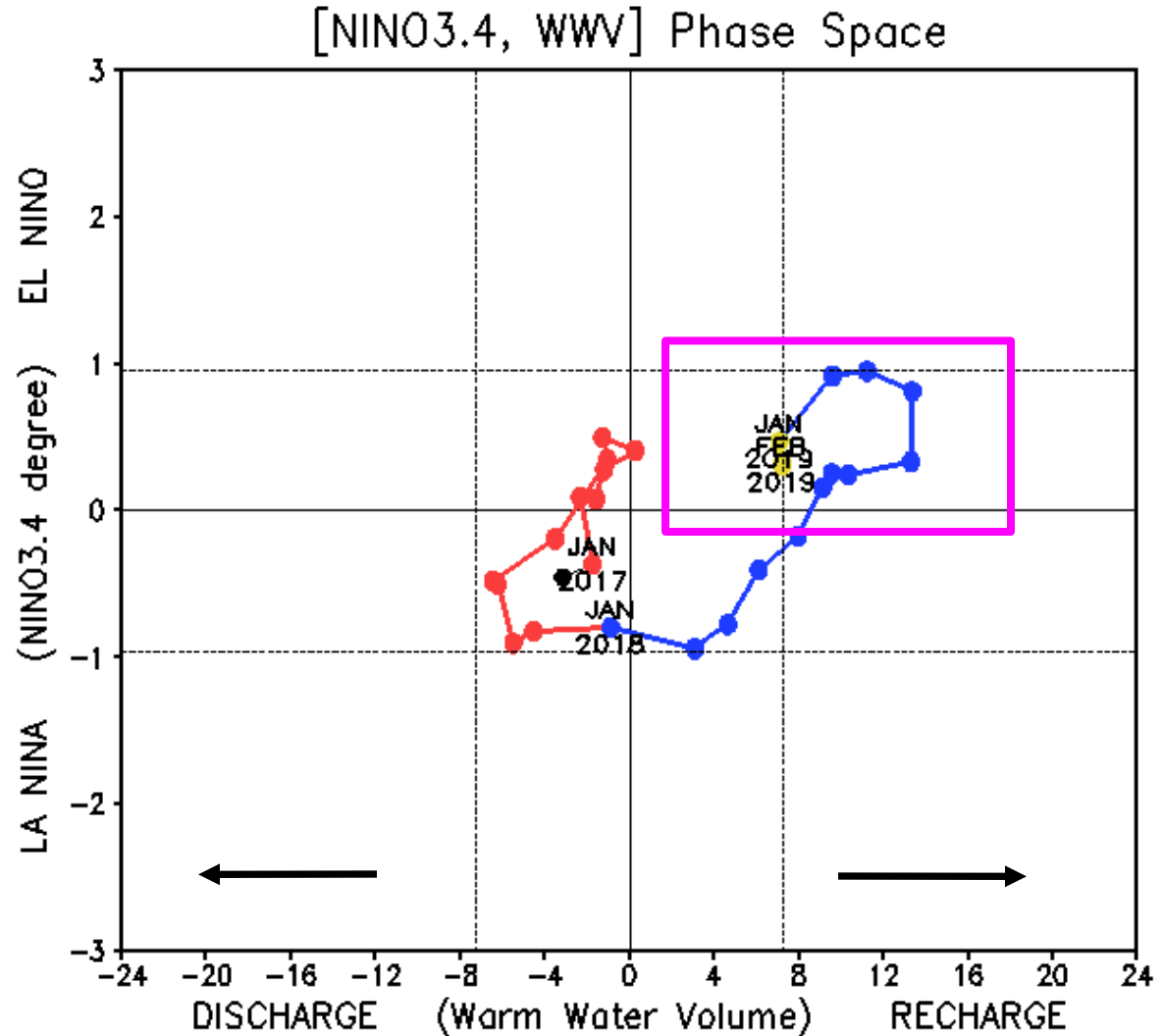
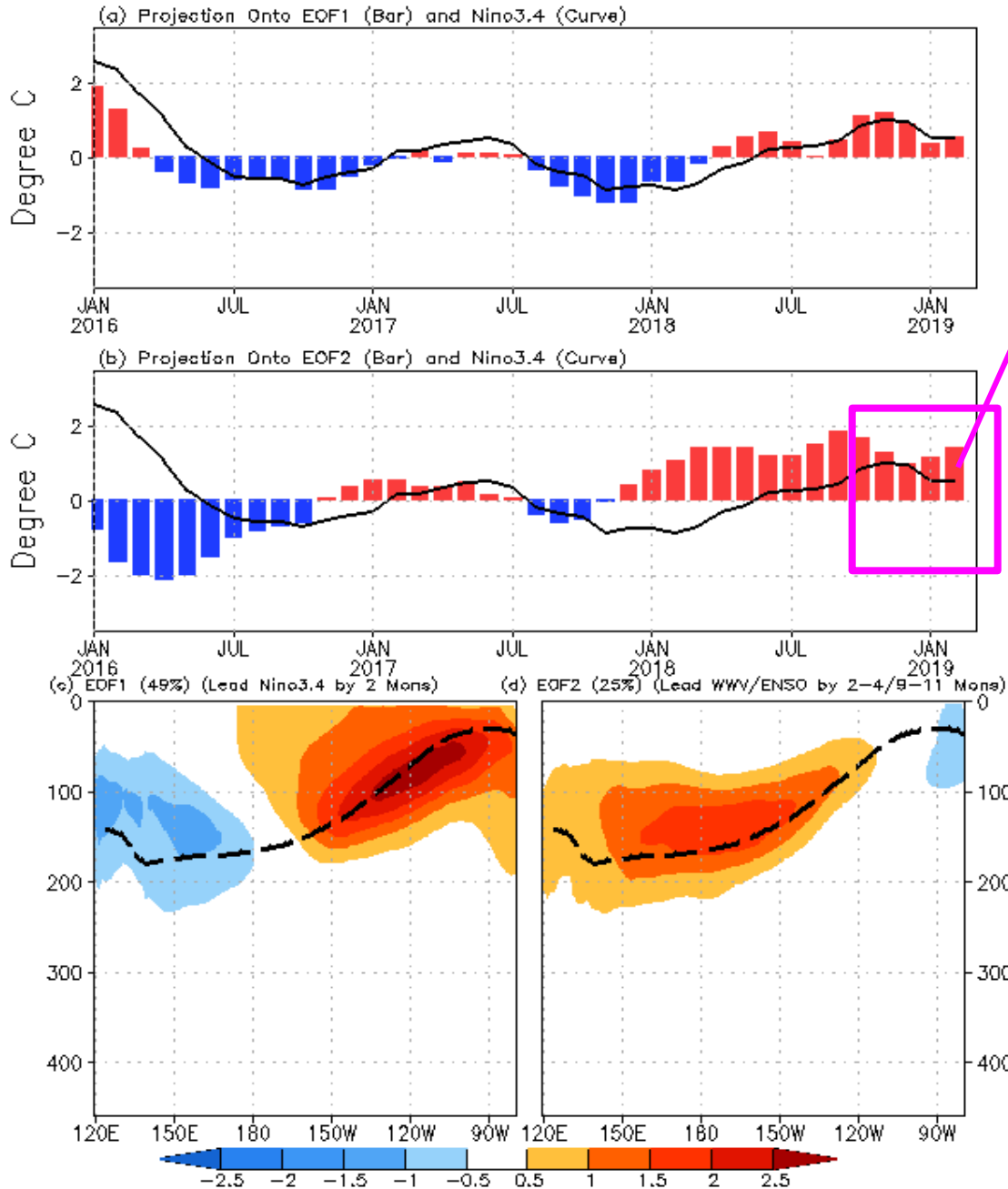


Fig. P3. Phase diagram of Warm Water Volume (WWV) and NINO 3.4 SST anomalies. WWV is the average of depth of 20°C in [120°E-80°W, 5°S-5°N] calculated with the NCEP's global ocean data assimilation system. Anomalies are departures from the 1981-2010 base period means.

GODAS OTA Projection & EOFs (0-459m, 2S-2N, 1979-2012)



Equatorial subsurface ocean temperature monitoring: ENSO was in a weak recharging phase in Jan-Feb 2019.

Projection of OTA onto EOF1 and EOF2 (2S-2N, 0-459m, 1979-2010)

EOF1: Tilt mode (ENSO peak phase);

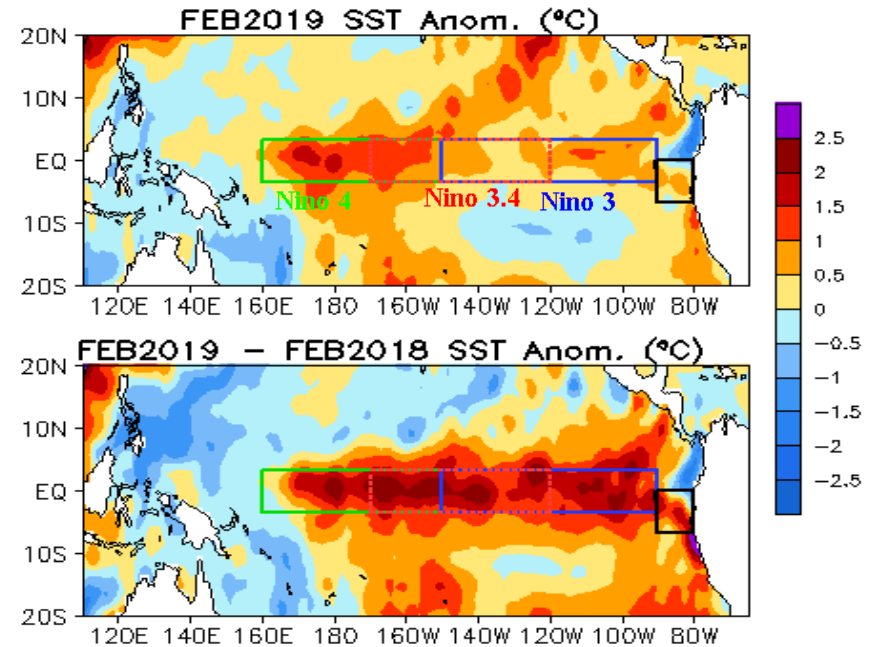
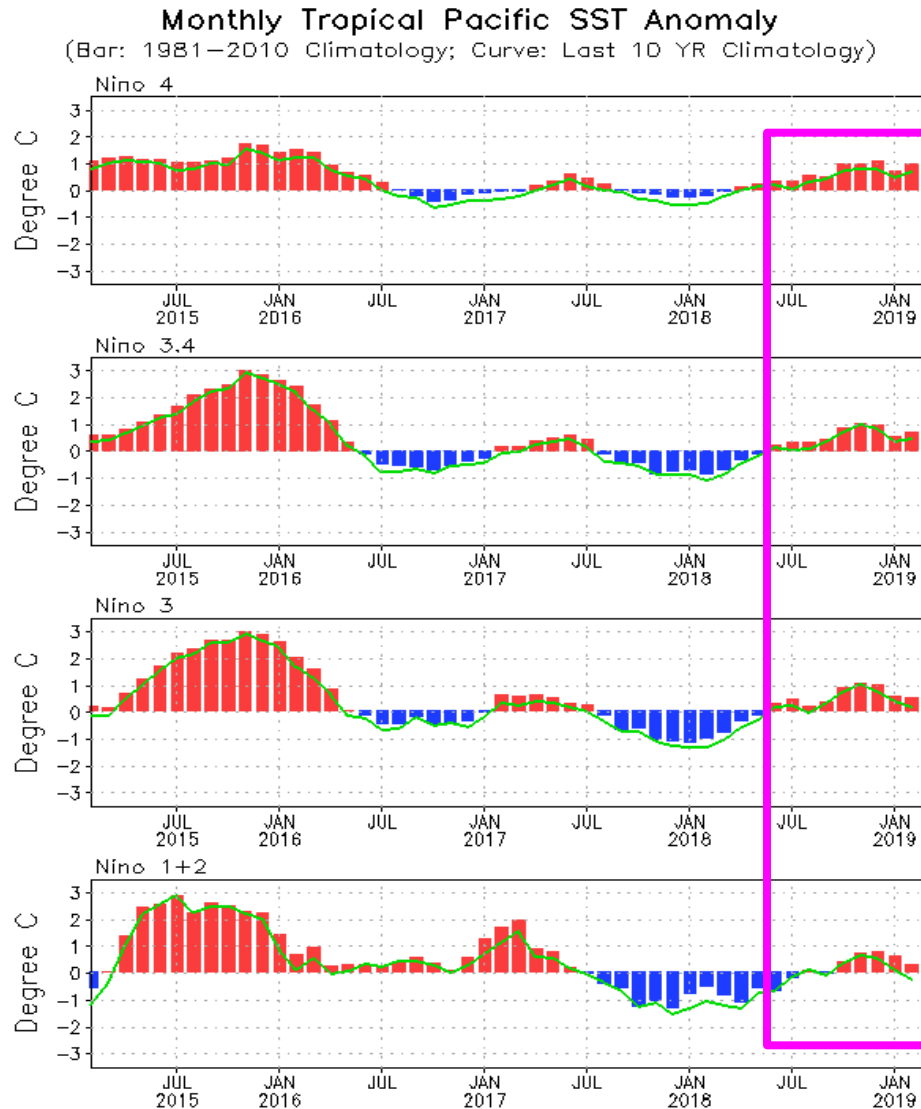
EOF2: WWV mode, Recharge/discharge oscillation (ENSO transition phase).

Recharge process: heat transport from outside of equator to equator : Negative -> positive phase of ENSO

Discharge process: heat transport from equator to outside of equator: Positive -> Negative phase of ENSO

For details, see:
 Kumar A, Z-Z Hu (2014) *Interannual and interdecadal variability of ocean temperature along the equatorial Pacific in conjunction with ENSO. Clim. Dyn.*, 42 (5-6), **1243-1258**. DOI: 10.1007/s00382-013-1721-0.

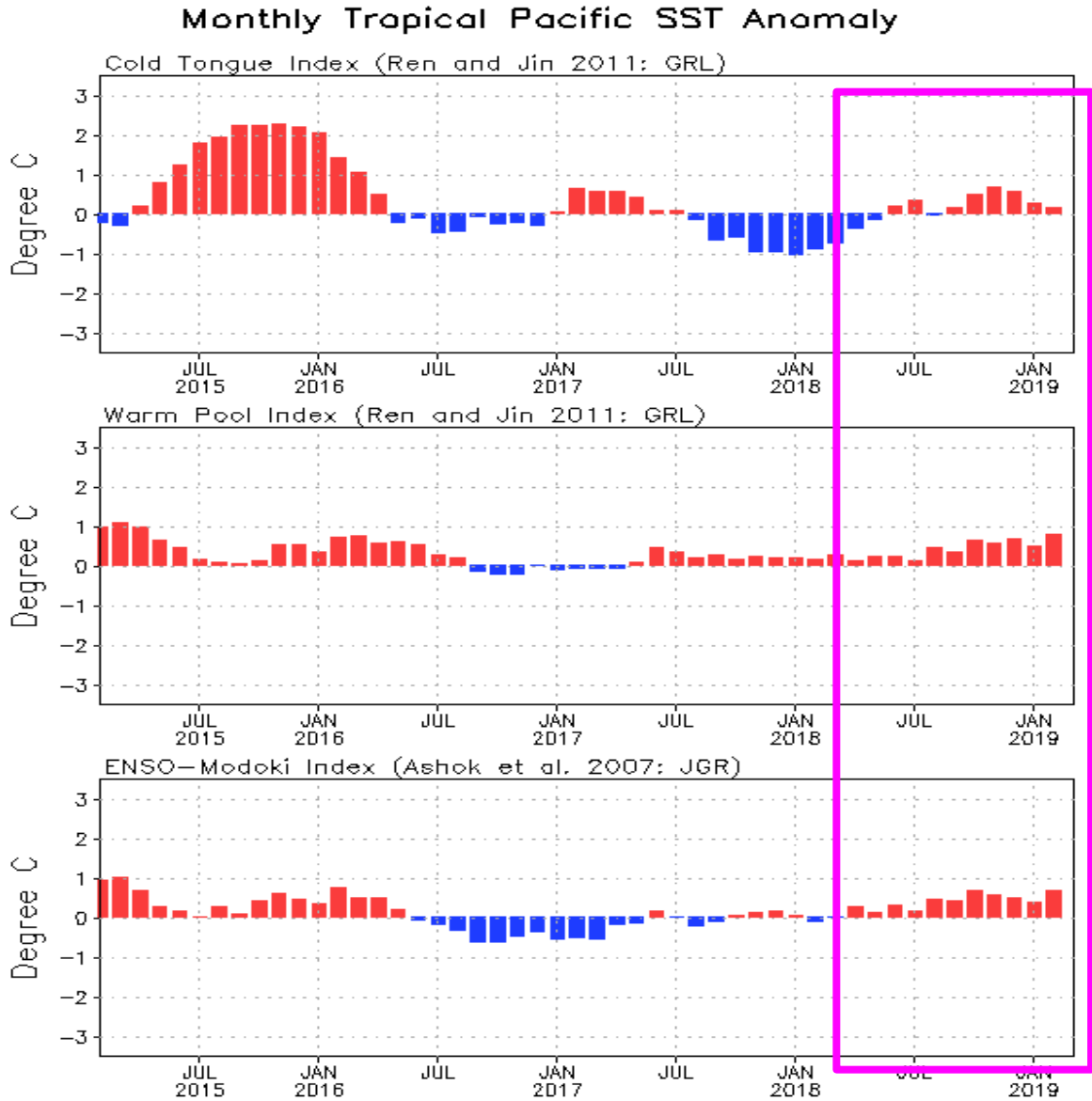
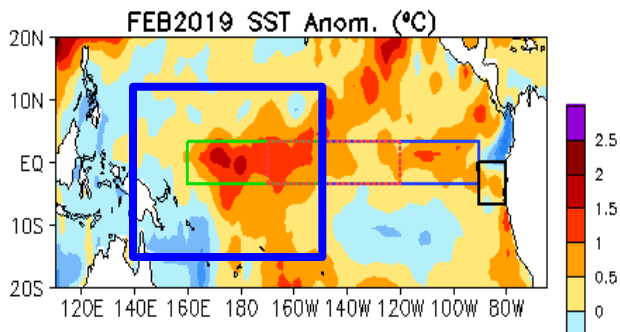
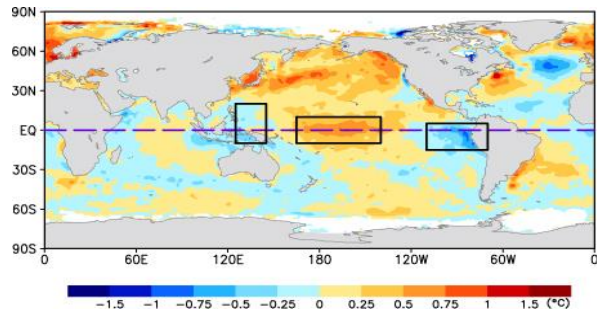
Evolution of Pacific NINO SST Indices



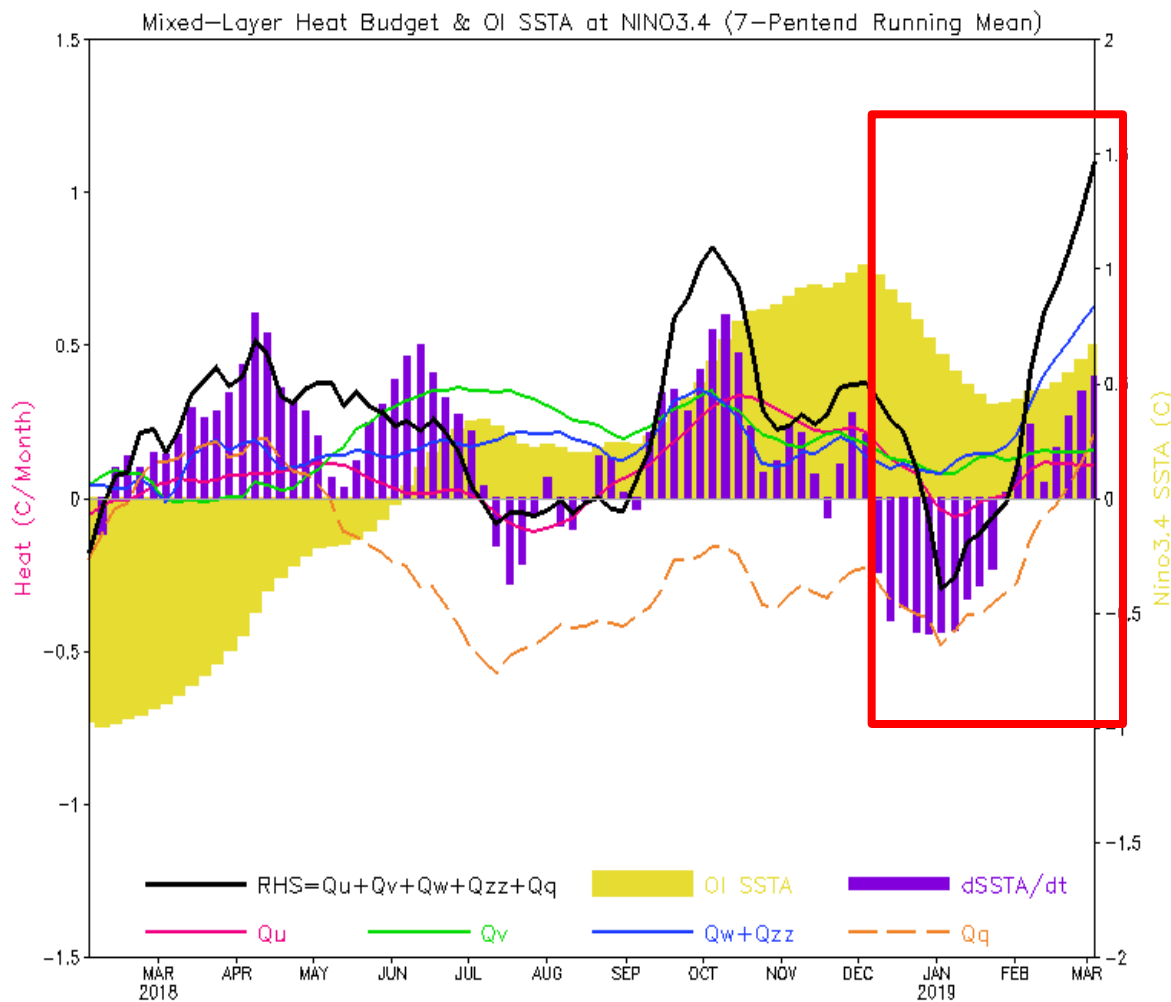
- Nino4 and Nino3.4 strengthened, and Nino3 and Nino1+2 weakened in Feb 2019.
- Nino3.4 = 0.66C in Feb 2019.
- Compared with last Feb, the central and eastern equatorial Pacific was much warmer in Feb 2019.
- The indices were calculated based on OISST. They may have some differences compared with those based on ERSST.v5.

Fig. P1a. Nino region indices, calculated as the area-averaged monthly mean sea surface temperature anomalies (°C) for the specified region. Data are derived from the NCEP OI SST analysis, and anomalies are departures from the 1981-2010 base period means.

Positive SSTAs were larger in the warm pool than in the cold tongue



NINO3.4 Heat Budget



- Both observed SSTA tendencies ($dSSTA/dt$; bar) and total heat budget (RHS; black line) in the Nino3.4 region were positive.

- All dynamical terms (Q_u , Q_v , Q_w+Q_{zz}) were positive while heat-flux term (Q_q) switched from negative to positive during Feb-Mar.

Huang, B., Y. Xue, X. Zhang, A. Kumar, and M. J. McPhaden, 2010 : The NCEP GODAS ocean analysis of the tropical Pacific mixed layer heat budget on seasonal to interannual time scales, *J. Climate.*, 23, 4901-4925.

Q_u : Zonal advection; Q_v : Meridional advection;

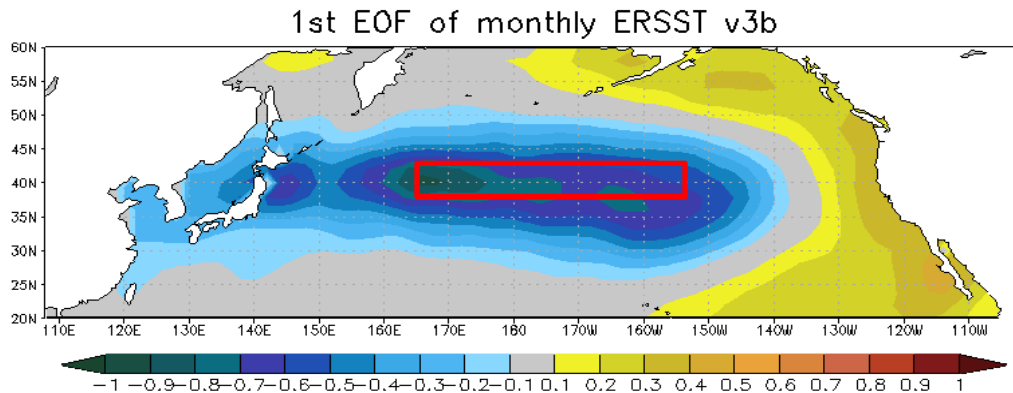
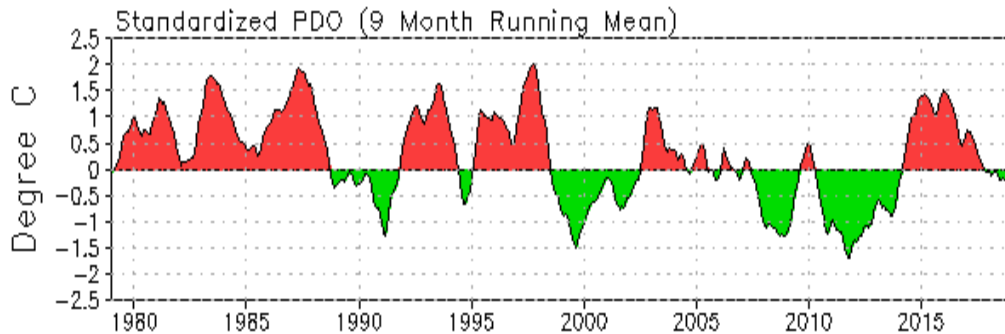
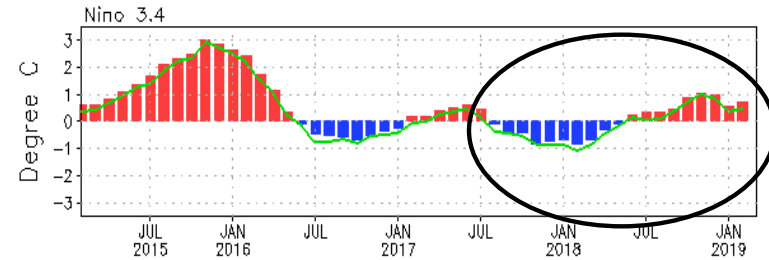
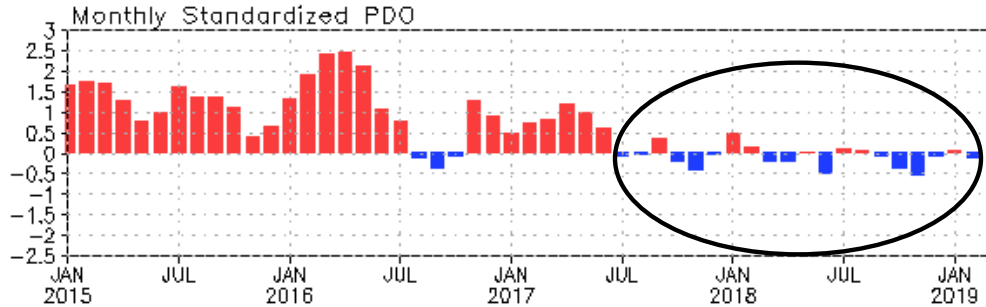
Q_w : Vertical entrainment; Q_{zz} : Vertical diffusion

Q_q : $(Q_{net} - Q_{open} + Q_{corr})/pcph$; $Q_{net} = SW + LW + LH + SH$;

Q_{open} : SW penetration; Q_{corr} : Flux correction due to relaxation to OI SST

North Pacific & Arctic Oceans

PDO index



- The PDO index was small since Jul 2017 with PDOI=-0.1 in Feb 2019.

- Statistically, ENSO leads PDO by 3-4 months, may through atmospheric bridge.

- During the last 1~2 years, ENSO and PDO seem disconnected.

- Pacific Decadal Oscillation is defined as the 1st EOF of monthly ERSST v3b in the North Pacific for the period 1900-1993. PDO index is the standardized projection of the monthly SST anomalies onto the 1st EOF pattern.

- The PDO index differs slightly from that of JISAO, which uses a blend of UKMET and OIv1 and OIv2 SST.

North Pacific & Arctic Ocean: SST Anom., SST Anom. Tend., OLR, SLP, Sfc Rad, Sfc Flx

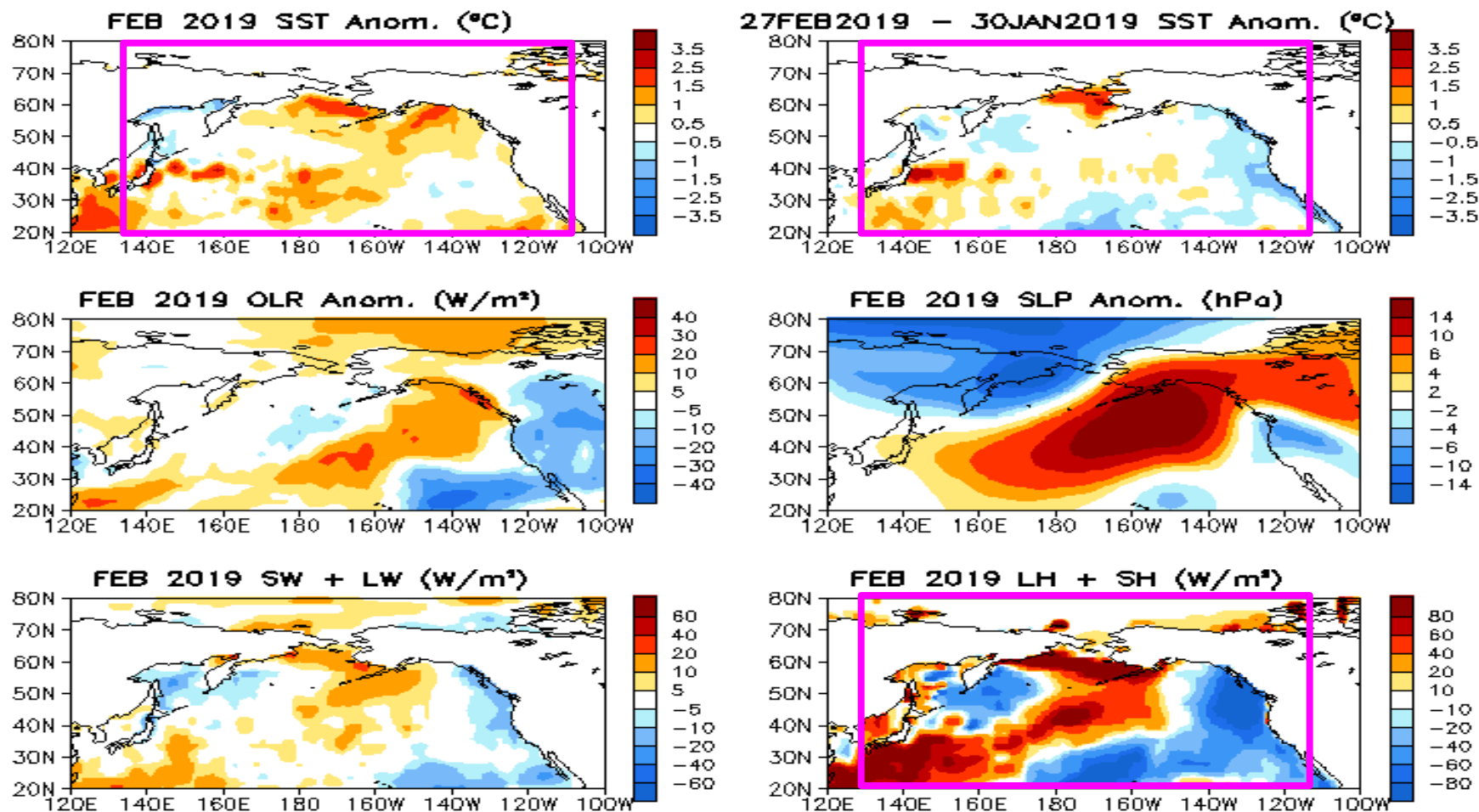
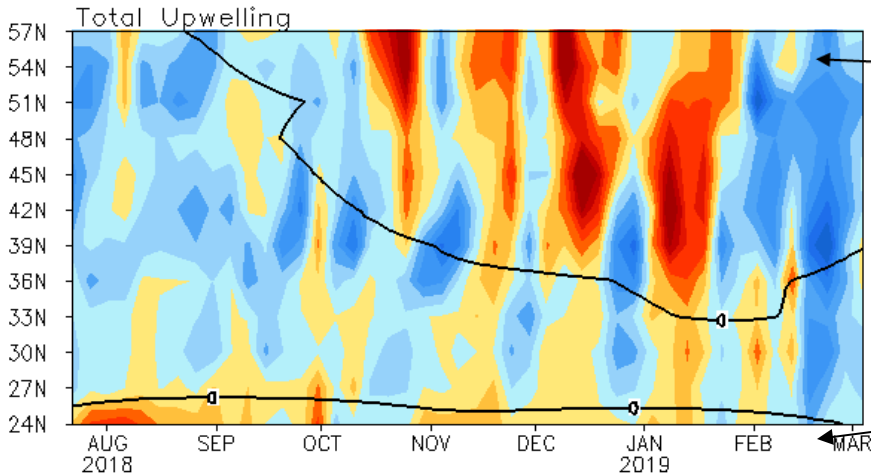


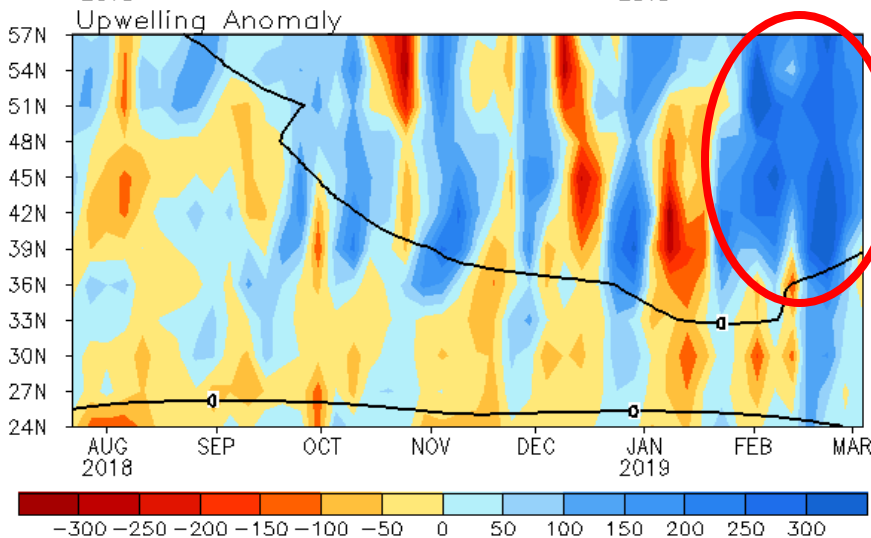
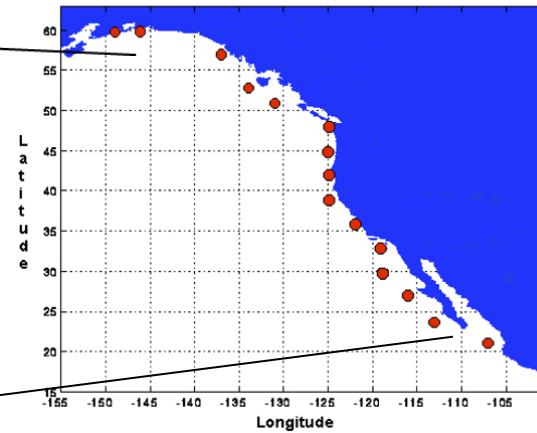
Fig. NP1. Sea surface temperature (SST) anomalies (top-left), anomaly tendency (top-right), Outgoing Long-wave Radiation (OLR) anomalies (middle-left), sea surface pressure anomalies (middle-right), sum of net surface short- and long-wave radiation anomalies (bottom-left), sum of latent and sensible heat flux anomalies (bottom-right). SST are derived from the NCEP OI SST analysis, OLR from the NOAA 18 AVHRR IR window channel measurements by NESDIS, sea surface pressure and surface radiation and heat fluxes from the NCEP CDAS. Anomalies are departures from the 1981-2010 base period means.

North America Western Coastal Upwelling

Pentad Coastal Upwelling for West Coast North America
($\text{m}^3/\text{s}/100\text{m}$ coastline)



Standard Positions of Upwelling Index Calculations



- Recently, strong anomalous upwelling presented in Feb 2019, may be associated with positive SLP anomalies along the coast.

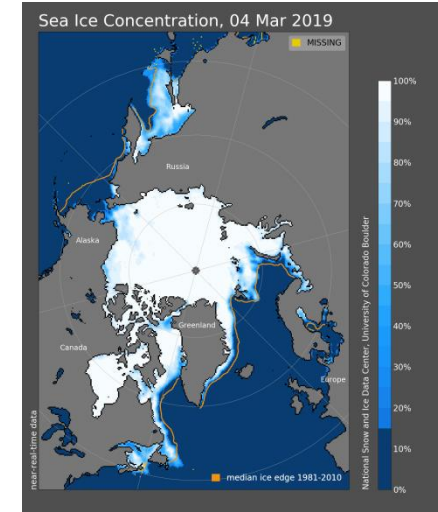
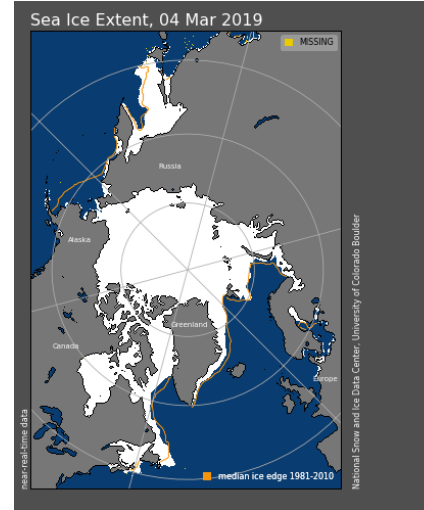
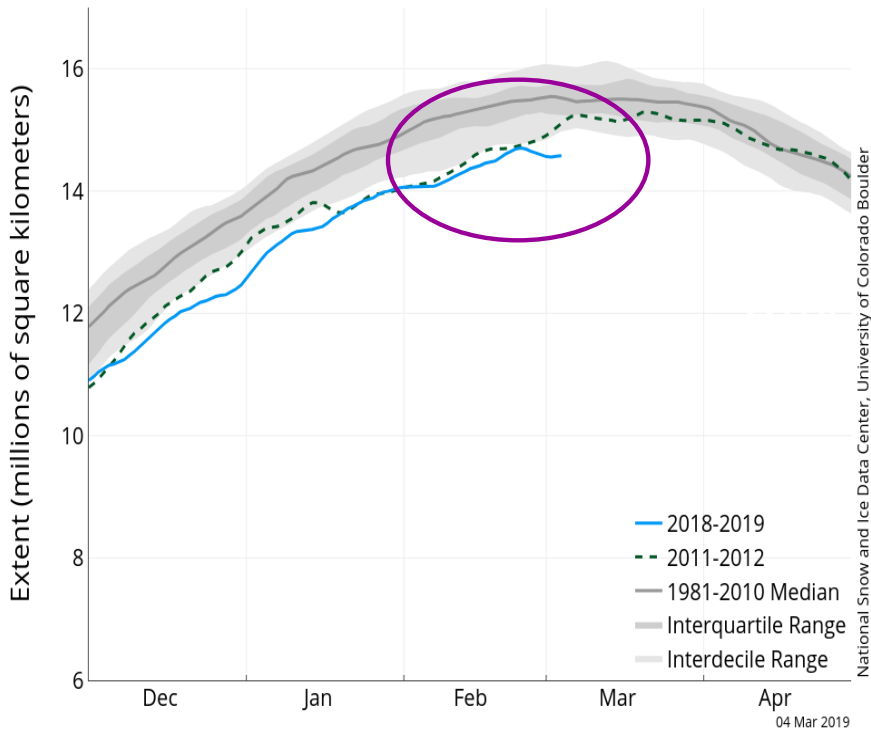
Fig. NP2. Total (top) and anomalous (bottom) upwelling indices at the 15 standard locations for the western coast of North America. Upwelling indices are derived from the vertical velocity of the NCEP's global ocean data assimilation system, and are calculated as integrated vertical volume transport at 50 meter depth from each location to its nearest coast point ($\text{m}^3/\text{s}/100\text{m}$ coastline). Anomalies are departures from the 1981-2010 base period pentad means.

- Area below (above) black line indicates climatological upwelling (downwelling) season.
- Climatologically upwelling season progresses from March to July along the west coast of North America from 36°N to 57°N .

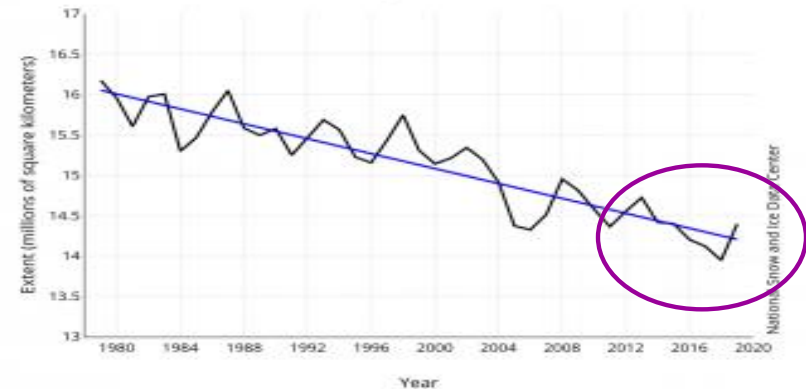
Arctic Sea Ice

National Snow and Ice Data Center
<http://nsidc.org/arcticseaicenews/index.html>

Arctic Sea Ice Extent
 (Area of ocean with at least 15% sea ice)



Average Monthly Arctic Sea ice Extent
 February 1979 - 2019



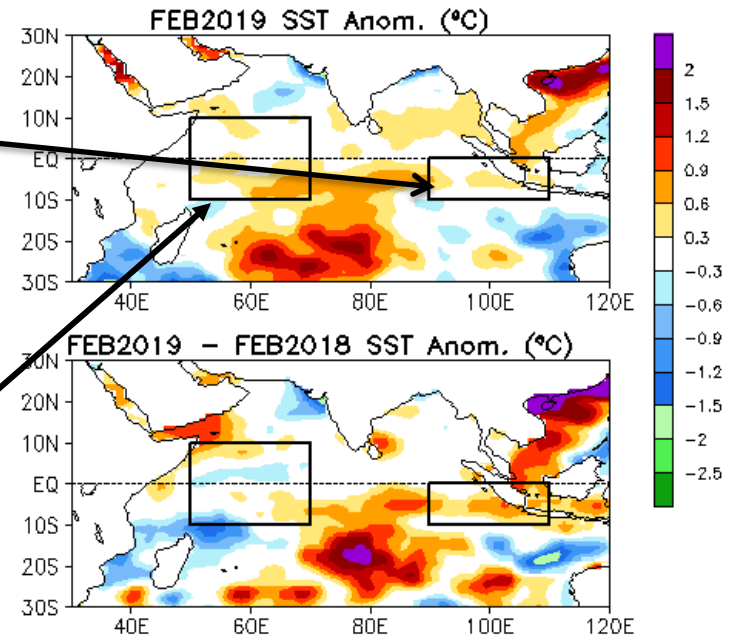
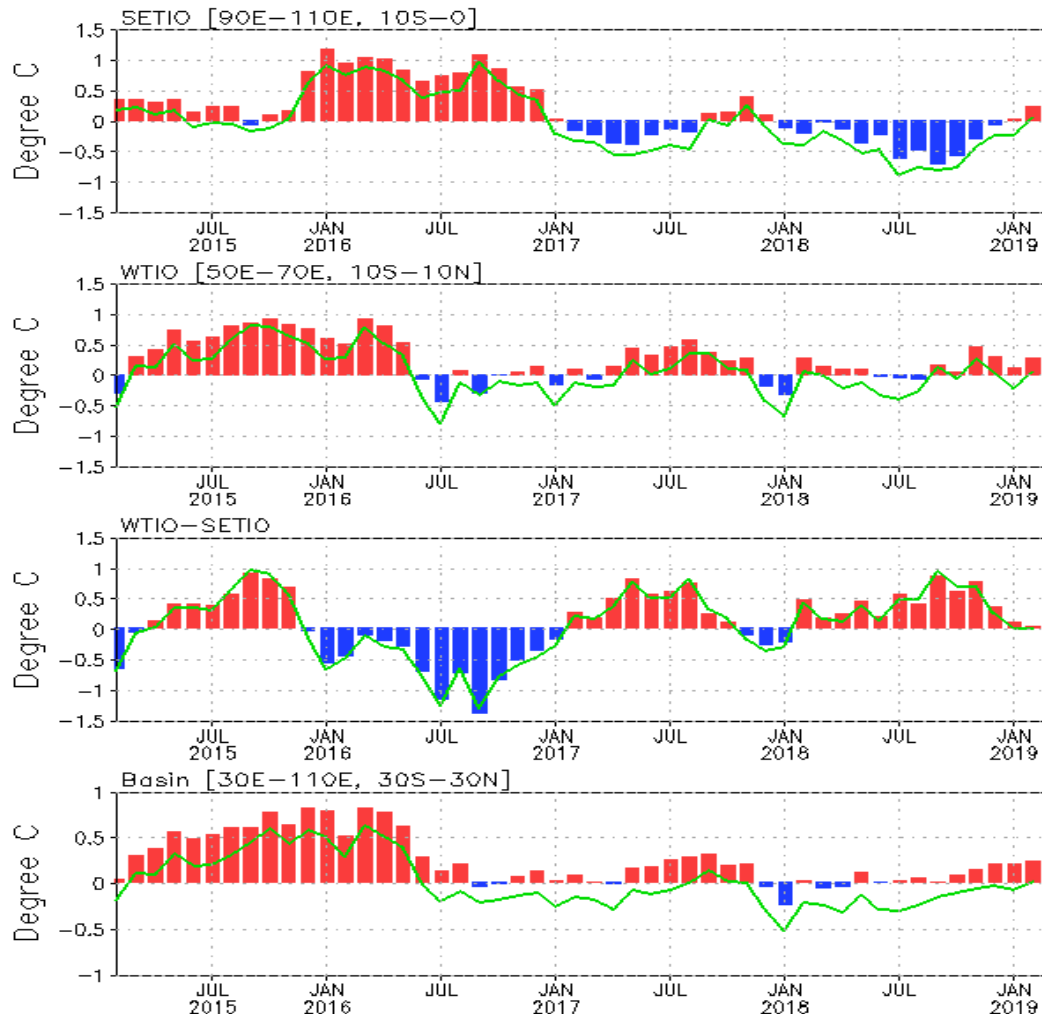
- Arctic sea ice extent for Feb 2019 was the 7th lowest in the satellite record for the month, tying with 2015.
 - So far this winter, sea ice extent has remained above the 2017 record low maximum.

Indian Ocean

Evolution of Indian Ocean SST Indices

Monthly Tropical Indian SST Anomaly

(Bar: 1981–2010 Climatology; Curve: Last 10 YR Climatology)



- Overall, tropical SSTAs were above normal.

Fig. I1a. Indian Ocean Dipole region indices, calculated as the area-averaged monthly mean sea surface temperature anomalies (°C) for the SETIO [90°E-110°E, 10°S-0] and WTIO [50°E-70°E, 10°S-10°N] regions, and Dipole Mode Index, defined as differences between WTIO and SETIO. Data are derived from the NCEP OI SST analysis, and anomalies are departures from the 1981-2010 base period means.

Tropical Indian: SST Anom., SST Anom. Tend., OLR, Sfc Rad, Sfc Flx, 925-mb & 200-mb Wind Anom.

- Overall SSTAs were small in the tropics.
- SSTA tendency was partially determined by heat flux.
- Convections were enhanced over the central basin.

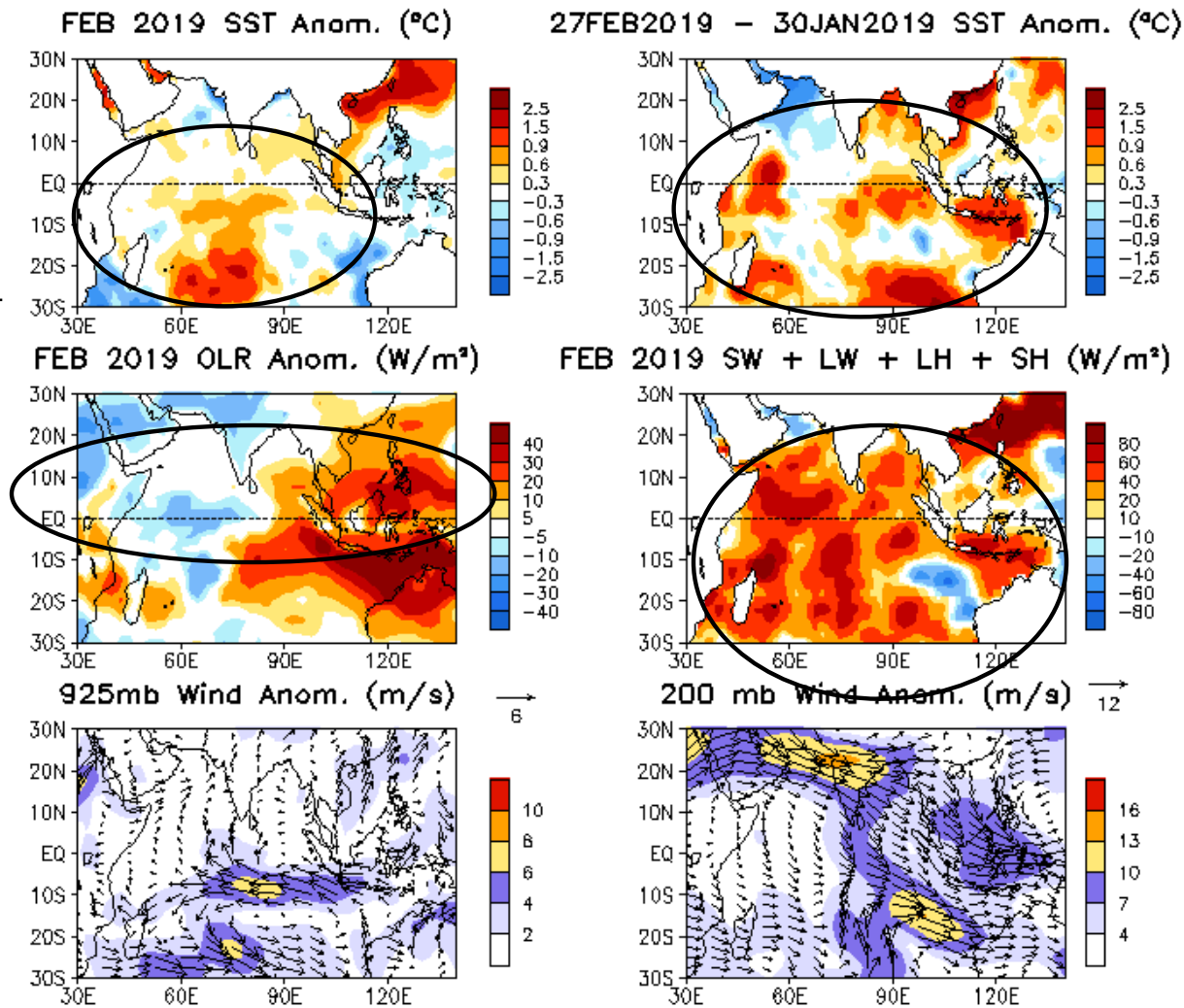


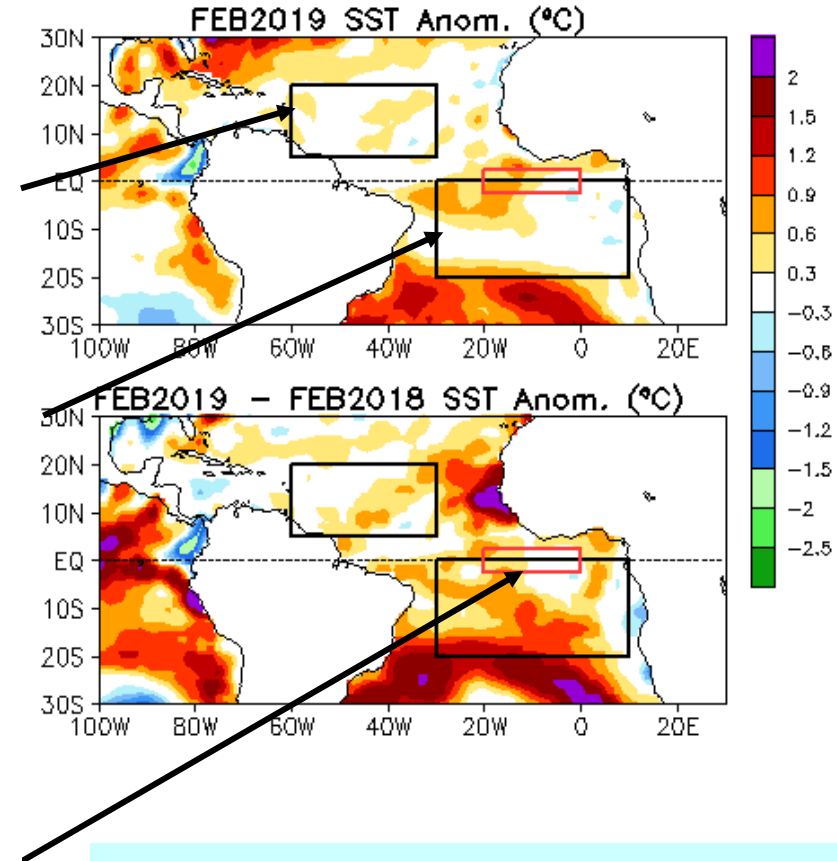
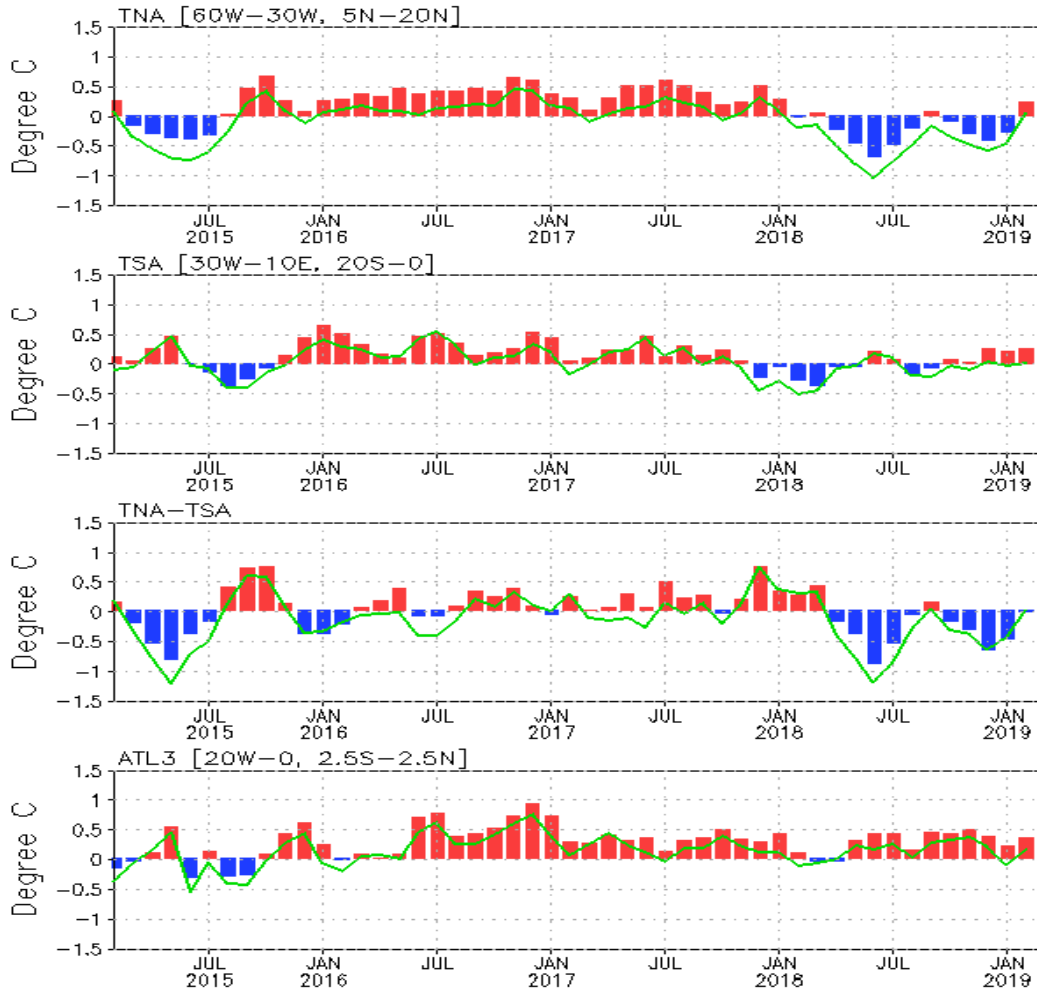
Fig. 12. Sea surface temperature (SST) anomalies (top-left), anomaly tendency (top-right), Outgoing Long-wave Radiation (OLR) anomalies (middle-left), sum of net surface short- and long-wave radiation, latent and sensible heat flux anomalies (middle-right), 925-mb wind anomaly vector and its amplitude (bottom-left), 200-mb wind anomaly vector and its amplitude (bottom-right). SST are derived from the NCEP OI SST analysis, OLR from the NOAA 18 AVHRR IR window channel measurements by NESDIS, winds and surface radiation and heat fluxes from the NCEP CDAS. Anomalies are departures from the 1981-2010 base period means.

Tropical and North Atlantic Ocean

Evolution of Tropical Atlantic SST Indices

Monthly Tropical Atlantic SST Anomaly

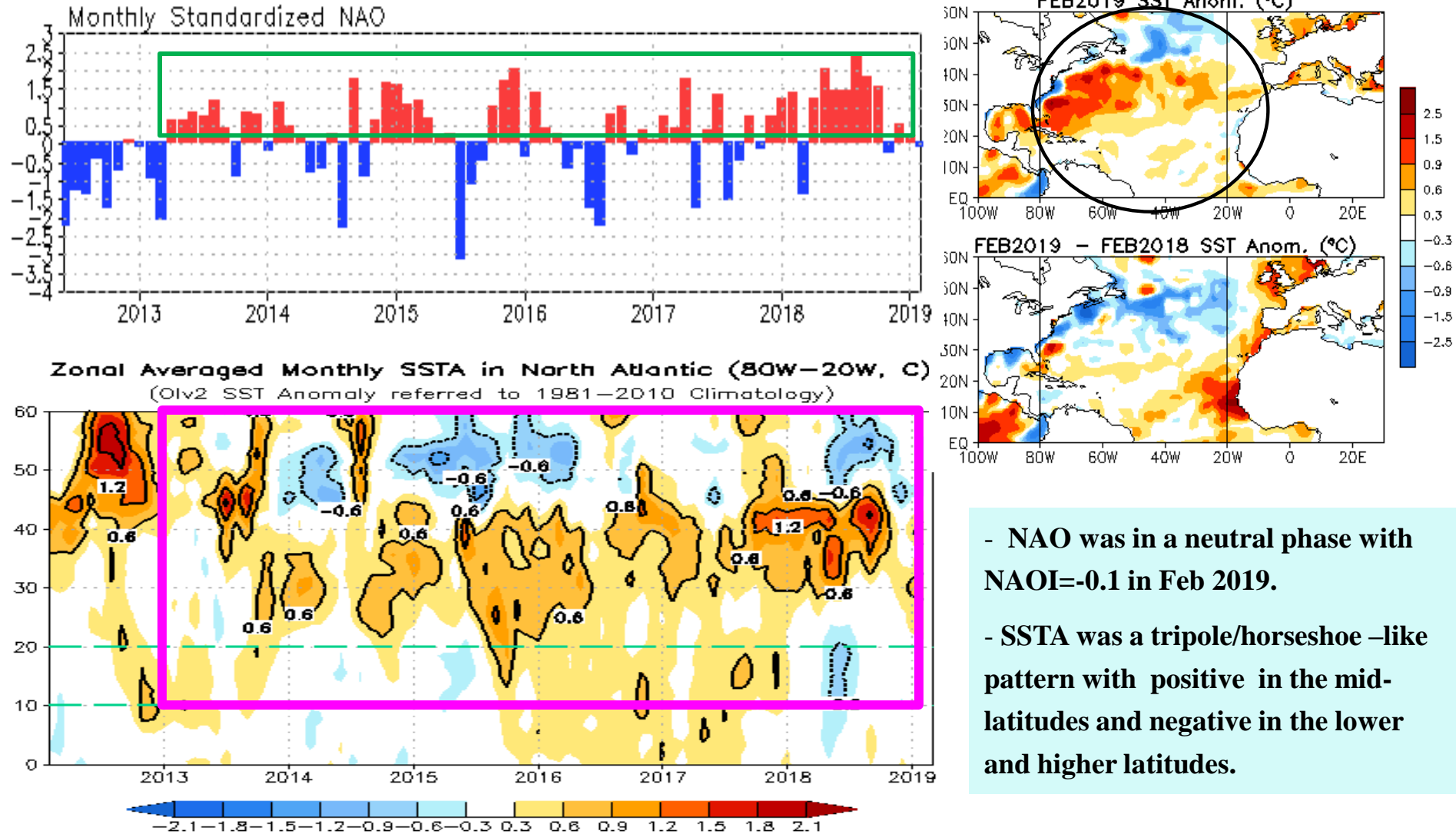
(Bar: 1981–2010 Climatology; Curve: Last 10 YR Climatology)



- All indices, except the dipole index, were positive in Feb 2019.

Fig. A1a. Tropical Atlantic Variability region indices, calculated as the area-averaged monthly mean sea surface temperature anomalies ($^{\circ}\text{C}$) for the TNA [60 $^{\circ}\text{W}$ -30 $^{\circ}\text{W}$, 5 $^{\circ}\text{N}$ -20 $^{\circ}\text{N}$], TSA [30 $^{\circ}\text{W}$ -10 $^{\circ}\text{E}$, 20 $^{\circ}\text{S}$ -0] and ATL3 [20 $^{\circ}\text{W}$ -0, 2.5 $^{\circ}\text{S}$ -2.5 $^{\circ}\text{N}$] regions, and Meridional Gradient Index, defined as differences between TNA and TSA. Data are derived from the NCEP OI SST analysis, and anomalies are departures from the 1981-2010 base period means.

NAO and SST Anomaly in North Atlantic

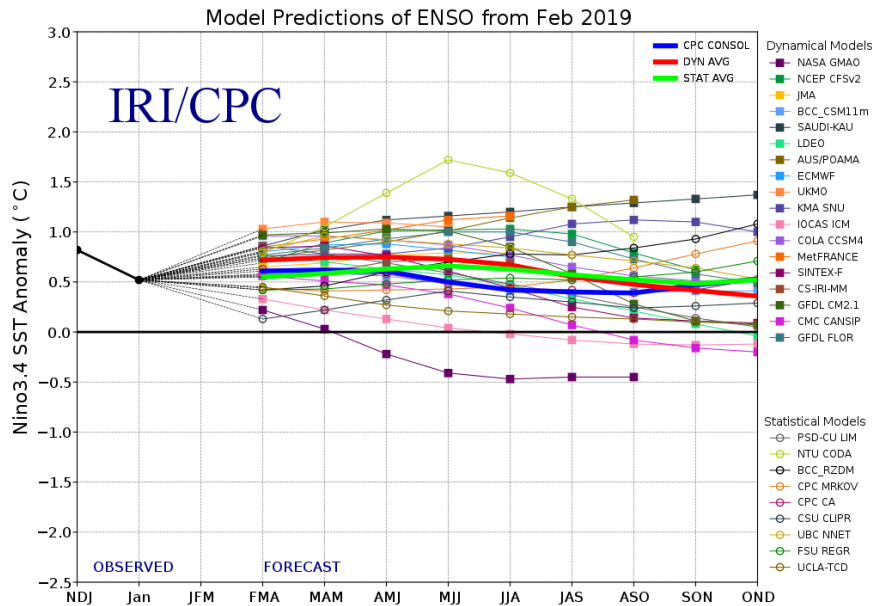


- NAO was in a neutral phase with NAOI=-0.1 in Feb 2019.
- SSTA was a tripole/horseshoe-like pattern with positive in the mid-latitudes and negative in the lower and higher latitudes.

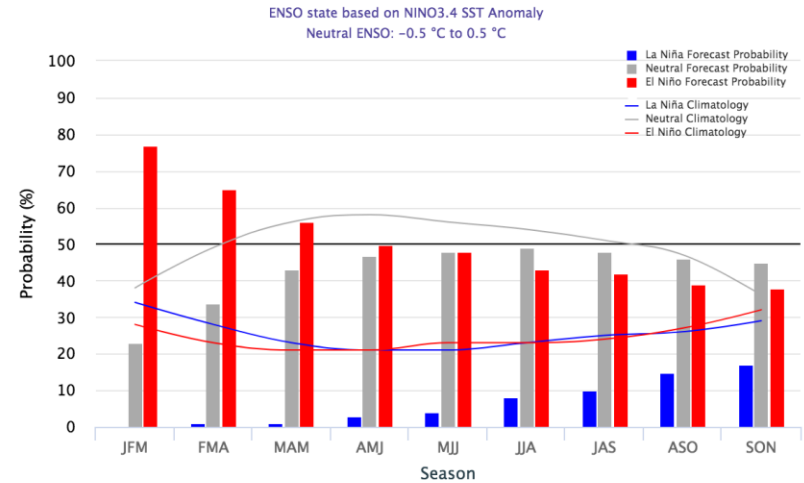
Fig. NA2. Monthly standardized NAO index (top) derived from monthly standardized 500-mb height anomalies obtained from the NCEP CDAS in 20°N-90°N (<http://www.cpc.ncep.noaa.gov>). Time-Latitude section of SST anomalies averaged between 80°W and 20°W (bottom). SST are derived from the NCEP OI SST analysis, and anomalies are departures from the 1981-2010 base period means.

ENSO and Global SST Predictions

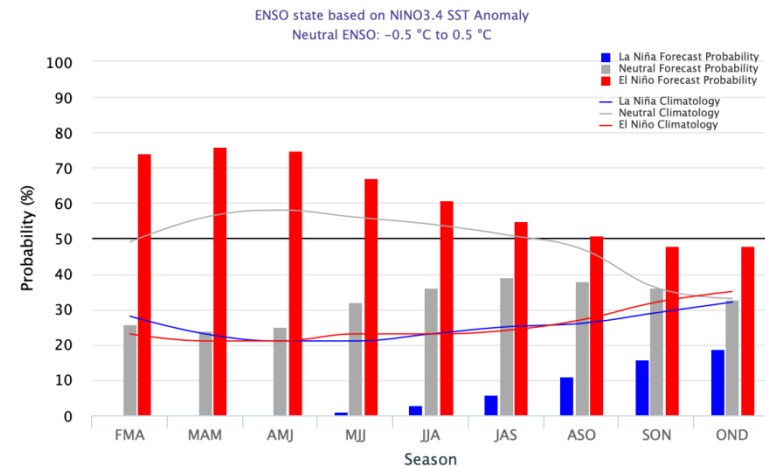
IRI NINO3.4 Forecast Plum



Early-February 2019 CPC/IRI Official Probabilistic ENSO Forecasts



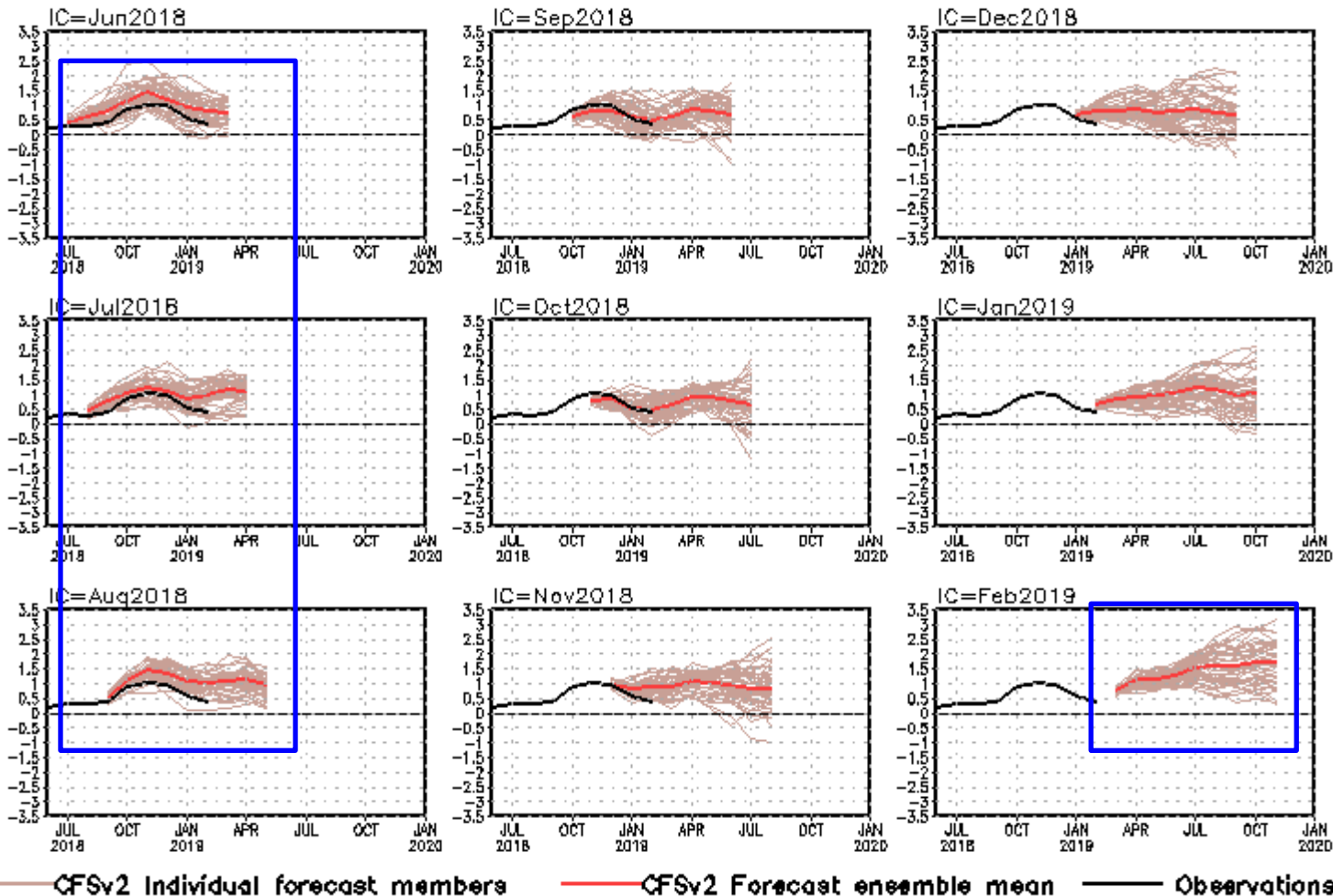
Mid-February 2019 IRI/CPC Model-Based Probabilistic ENSO Forecasts



- Some models predict continuation of El Niño in 2019.
- [NOAA “ENSO Diagnostic Discussion” on 14 Feb 2019](#) suggested that *“Weak El Niño conditions are present and are expected to continue through the Northern Hemisphere spring 2019 (~55% chance).”*

CFS Niño3.4 SST Predictions from Different Initial Months

NINO3.4 SST anomalies (K)

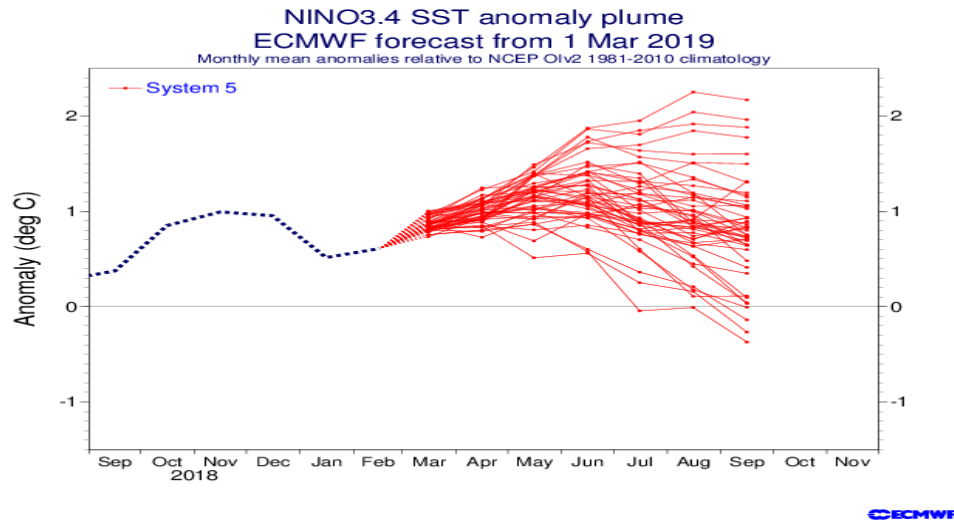


- Latest CFSv2 forecasts call for persistency of El Niño during summer-autumn 2019.
- CFSv2 predictions had warm biases with ICs in Jun-Aug 2018.

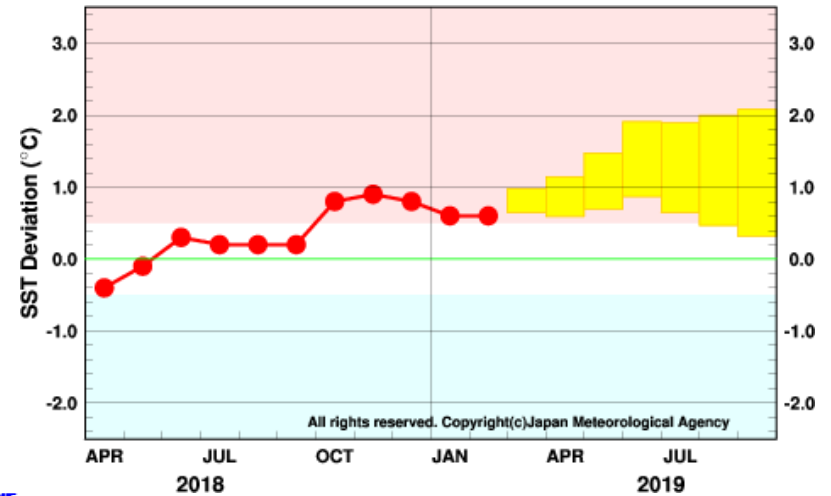
Fig. M1. CFS Niño3.4 SST prediction from the latest 9 initial months. Displayed are 40 forecast members (brown) made four times per day initialized from the last 10 days of the initial month (labelled as IC=MonthYear) as well as ensemble mean (blue) and observations (black). Anomalies were computed with respect to the 1981-2010 base period means.

Individual Model Forecasts: **El Nino or borderline El Nino**

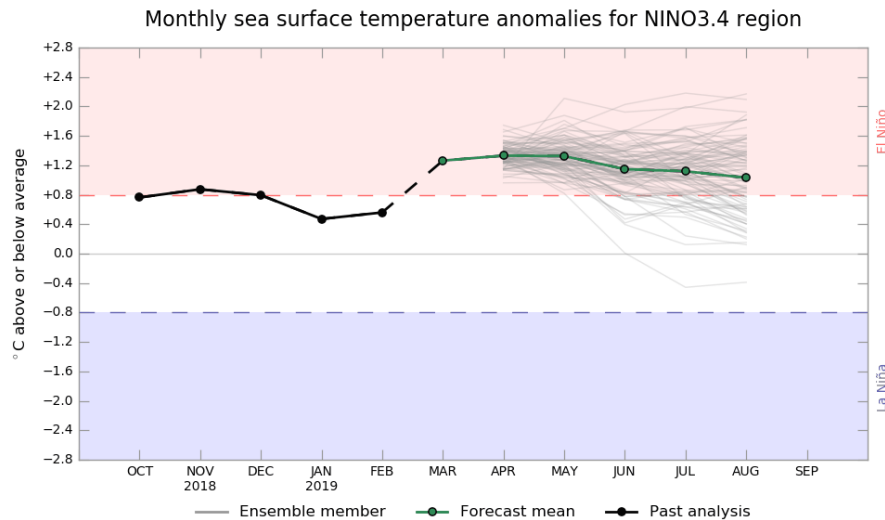
EC: Nino3.4, IC=01Mar 2019



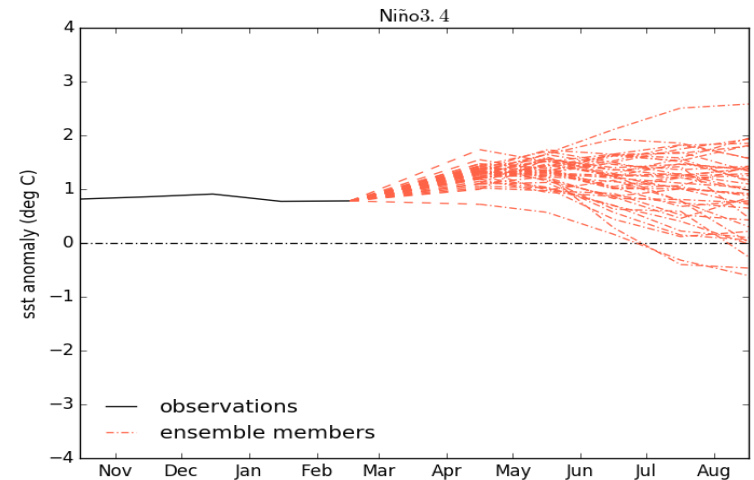
JMA: Nino3, Updated 11 Mar 2019



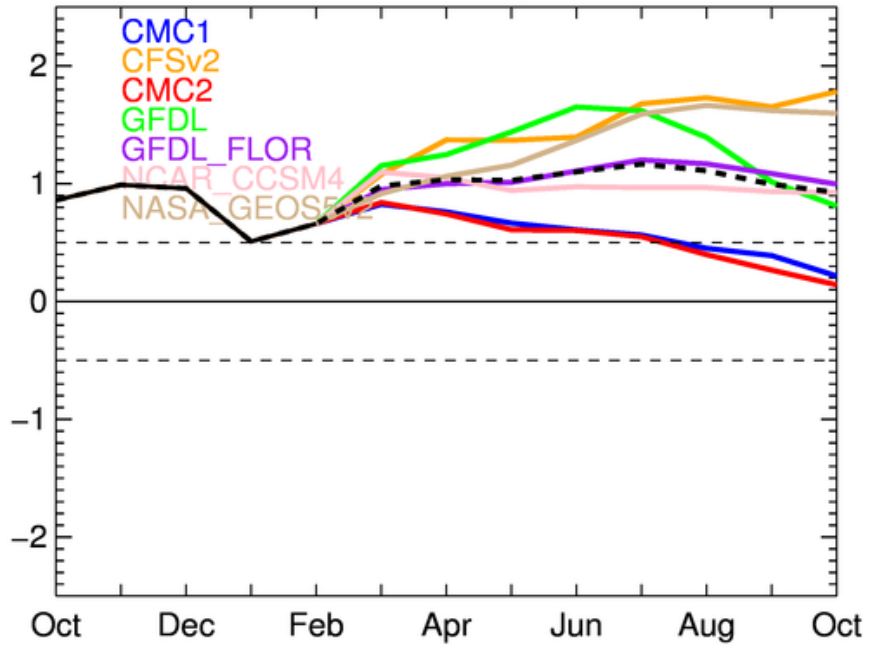
Australia: Nino3.4, Updated 02Mar 2019



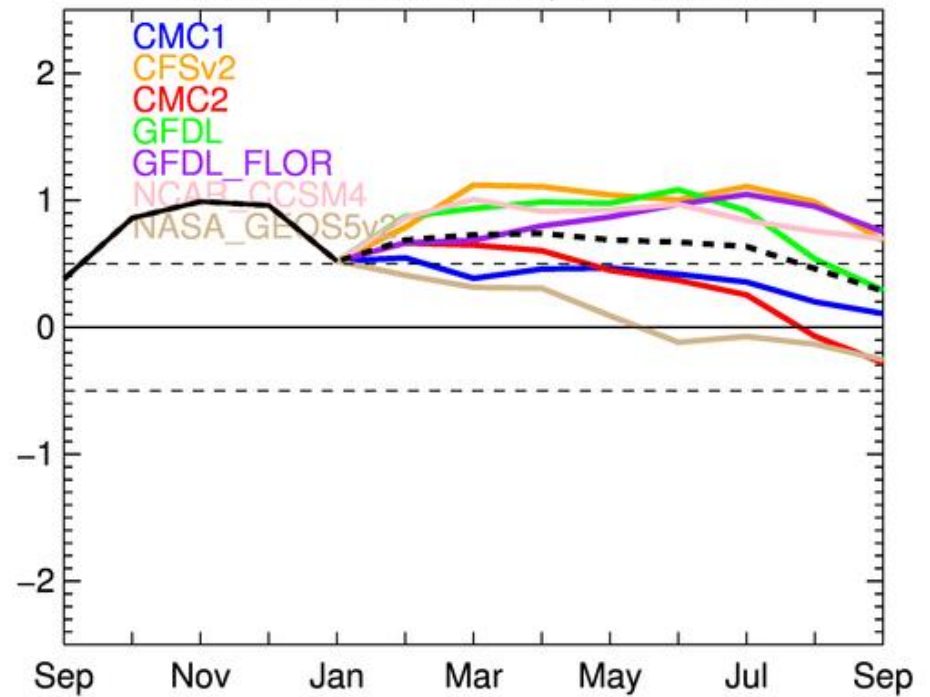
UKMO: Nino3.4, Updated 11 Mar 2019



NMME Nino3.4 Fcst, IC=201903



NMME Nino3.4 Fcst, IC=201902

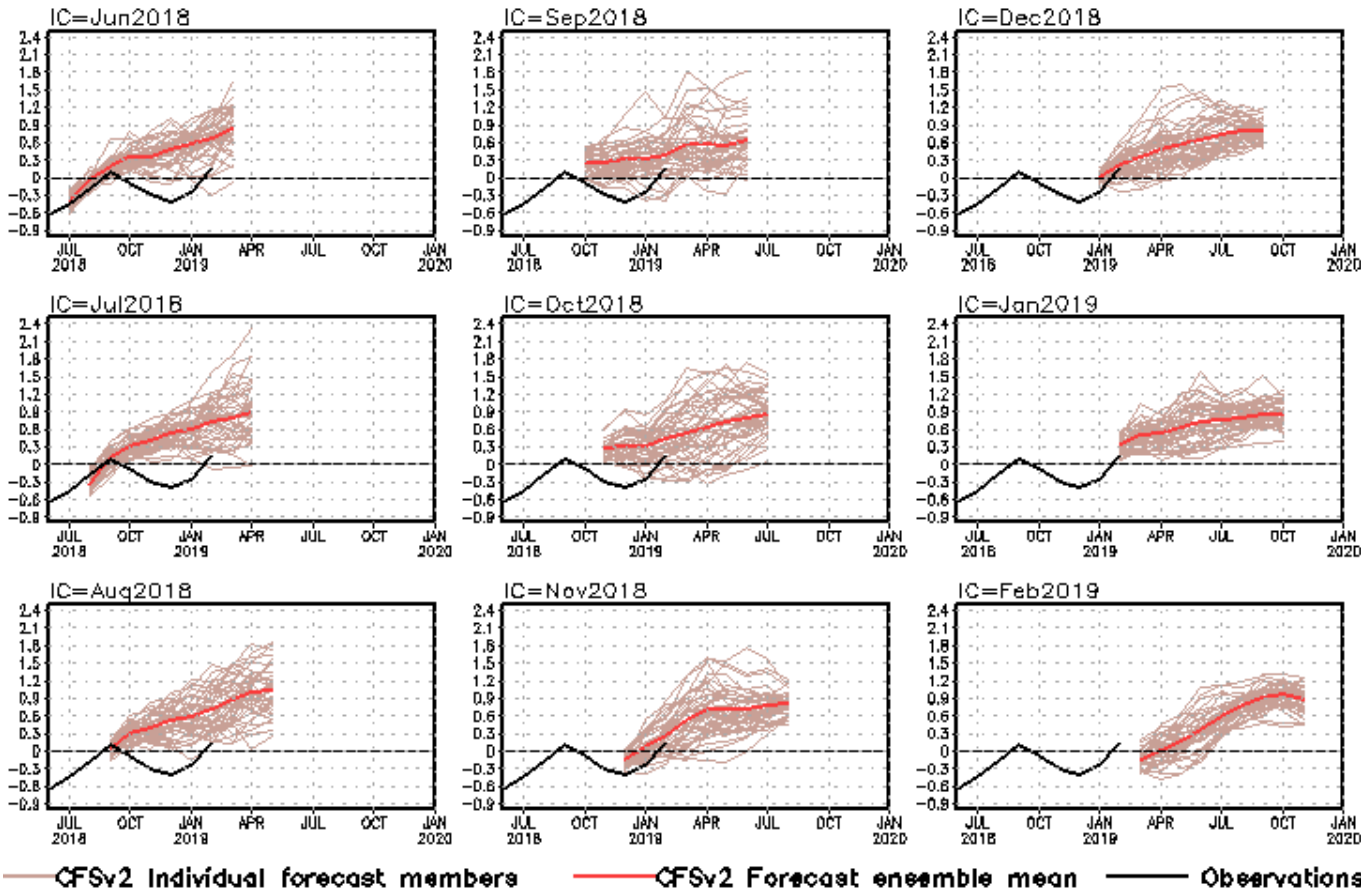


CFS Tropical North Atlantic (TNA) SST Predictions

from Different Initial Months

TNA is the SST anomaly averaged in the region of [60°W-30°W, 5°N-20°N].

Tropical N. Atlantic SST anomalies (K)



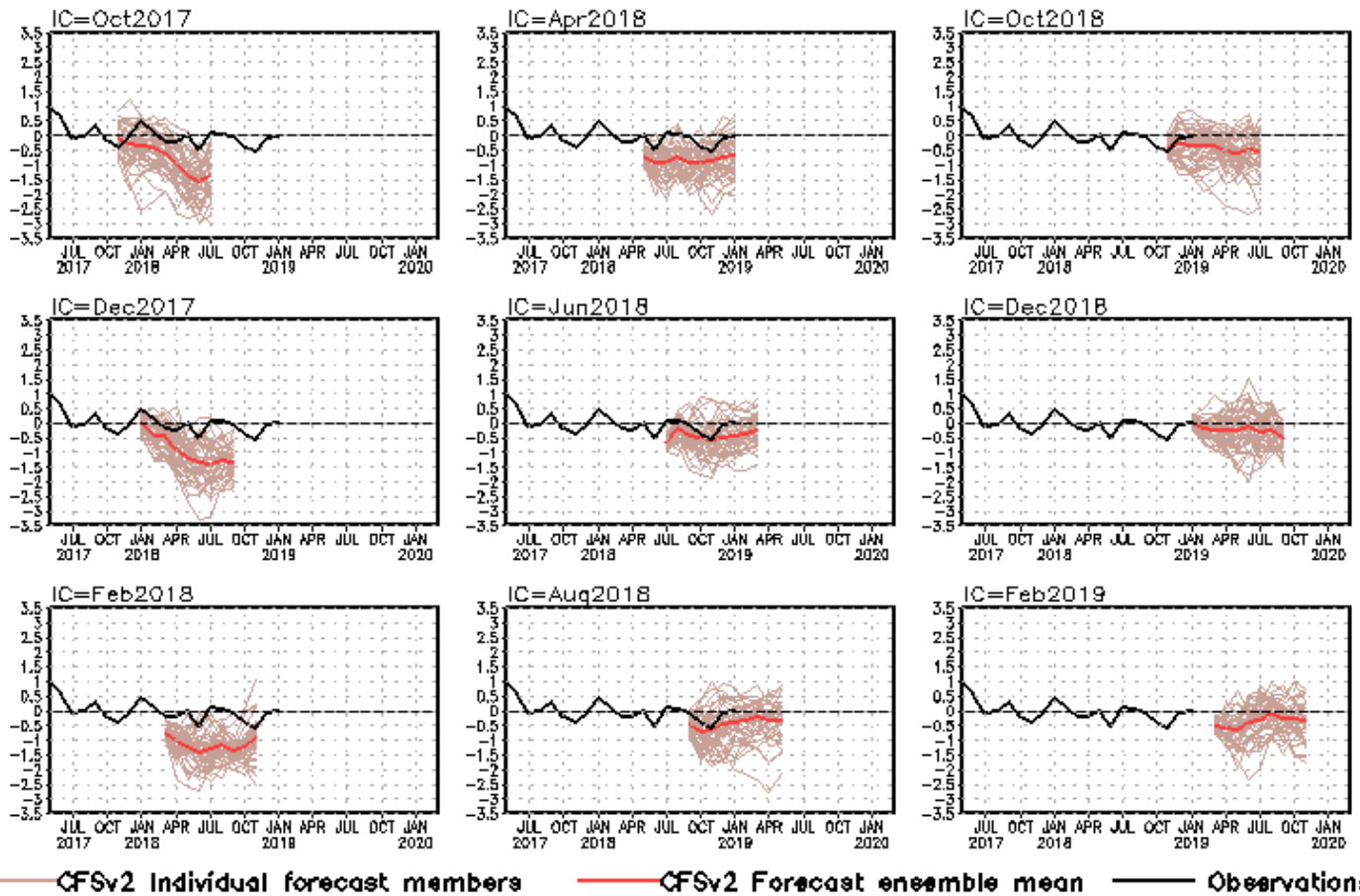
- Latest CFSv2 predictions call above normal SSTA in tropical N. Atlantic in summer-autumn 2019, consistent with the forecast warming in the tropical Pacific.

Fig. M3. CFS Tropical North Atlantic (TNA) SST predictions from the latest 9 initial months. Displayed are 40 forecast members (brown) made four times per day initialized from the last 10 days of the initial month (labelled as IC=MonthYear) as well as ensemble mean (blue) and observations (black). Anomalies were computed with respect to the 1981-2010 base period means.

CFS Pacific Decadal Oscillation (PDO) Index Predictions

from Different Initial Months

standardized PDO index



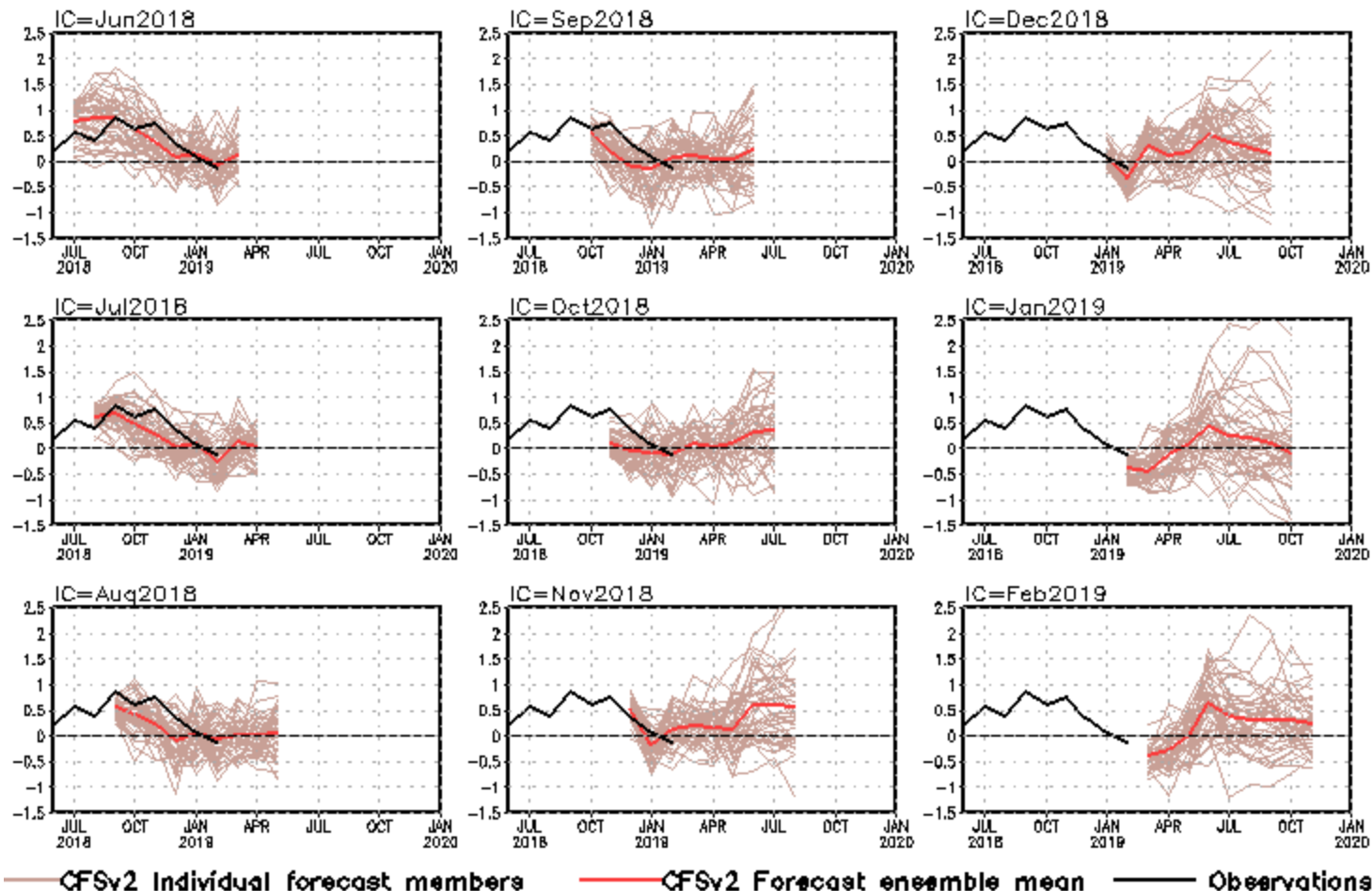
PDO is the first EOF of monthly ERSSTv3b anomaly in the region of [110°E-100°W, 20°N-60°N].
CFS PDO index is the standardized projection of CFS SST forecast anomalies onto the PDO EOF pattern.

- CFSv2 predicts a weak PDO in 2019.

Fig. M4. CFS Pacific Decadal Oscillation (PDO) index predictions from the latest 9 initial months. Displayed are 40 forecast members (brown) made four times per day initialized from the last 10 days of the initial month (labelled as IC=MonthYear) as well as ensemble mean (blue) and observations (black). Anomalies were computed with respect to the 1981-2010 base period means.

NCEP CFS DMI SST Predictions from Different Initial Months

Indian Ocean Dipole SST anomalies (K)

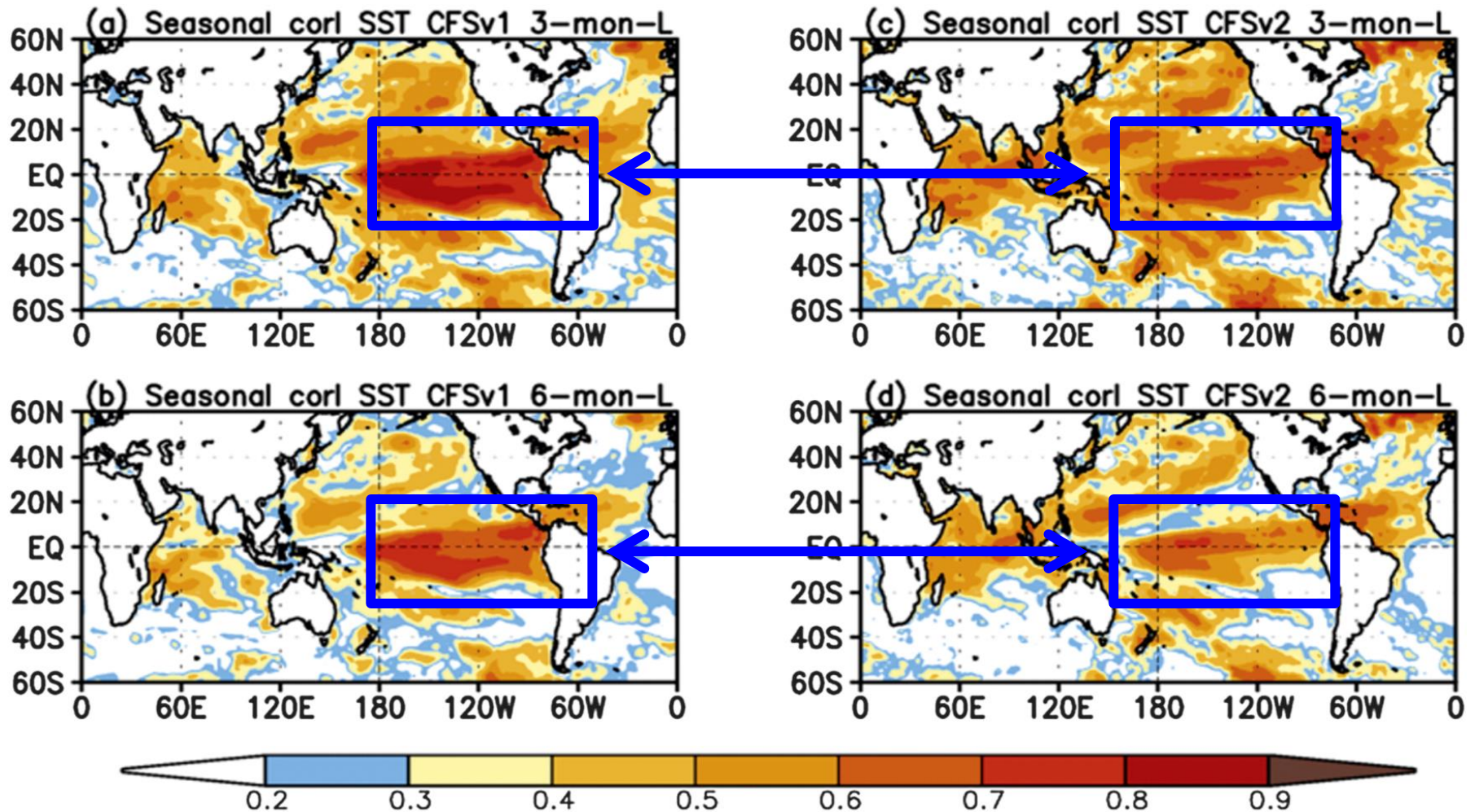


DMI = WTIO - SETIO
SETIO = SST anomaly in [90°E-110°E, 10°S-0]
WTIO = SST anomaly in [50°E-70°E, 10°S-10°N]

Fig. M2. CFS Dipole Model Index (DMI) SST predictions from the latest 9 initial months. Displayed are 40 forecast members (brown) made four times per day initialized from the last 10 days of the initial month (labelled as IC=MonthYear) as well as ensemble mean (blue) and observations (black). The hindcast climatology for 1981-2006 was removed, and replaced by corresponding observation climatology for the same period. Anomalies were computed with respect to the 1981-2010 base period means.

Challenges of Forecasting ENSO Cycle

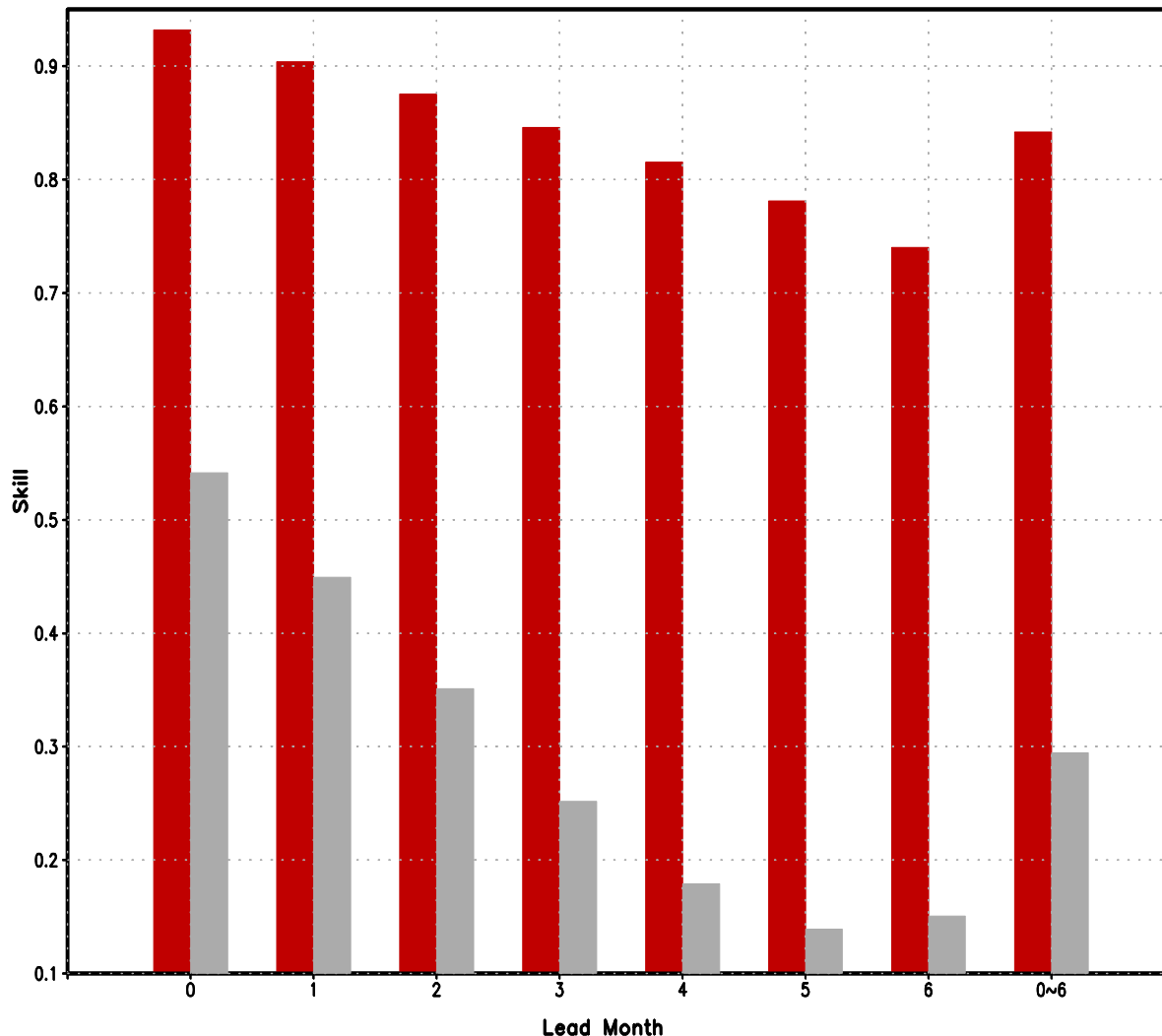
Hindcast skill of SSTA is the highest in the central and eastern tropical Pacific associated with ENSO ($>0.7\sim0.8$)



Anomaly correlation of 3-month-mean SSTA between model forecasts and observation: (a) 3-month lead CFSv1, (b) 6-month lead CFSv1, (c) 3-month lead CFSv2, and (d) 6-month lead CFSv2. Contours are plotted at an interval of 0.1.

(a) ENSO prediction skill is largely contributed by the skill in the periods with large Niño3.4 SSTA ($|\text{Niño3.4}| > 0.5$), consistent with previous works.

(b) It means that model can well capture the evolution of a happened cold/warm event around it peak, but it is hard to predict the initiation of the cold/warm event.



Skill varies with lead time and ENSO or ENSO-neutral in IC

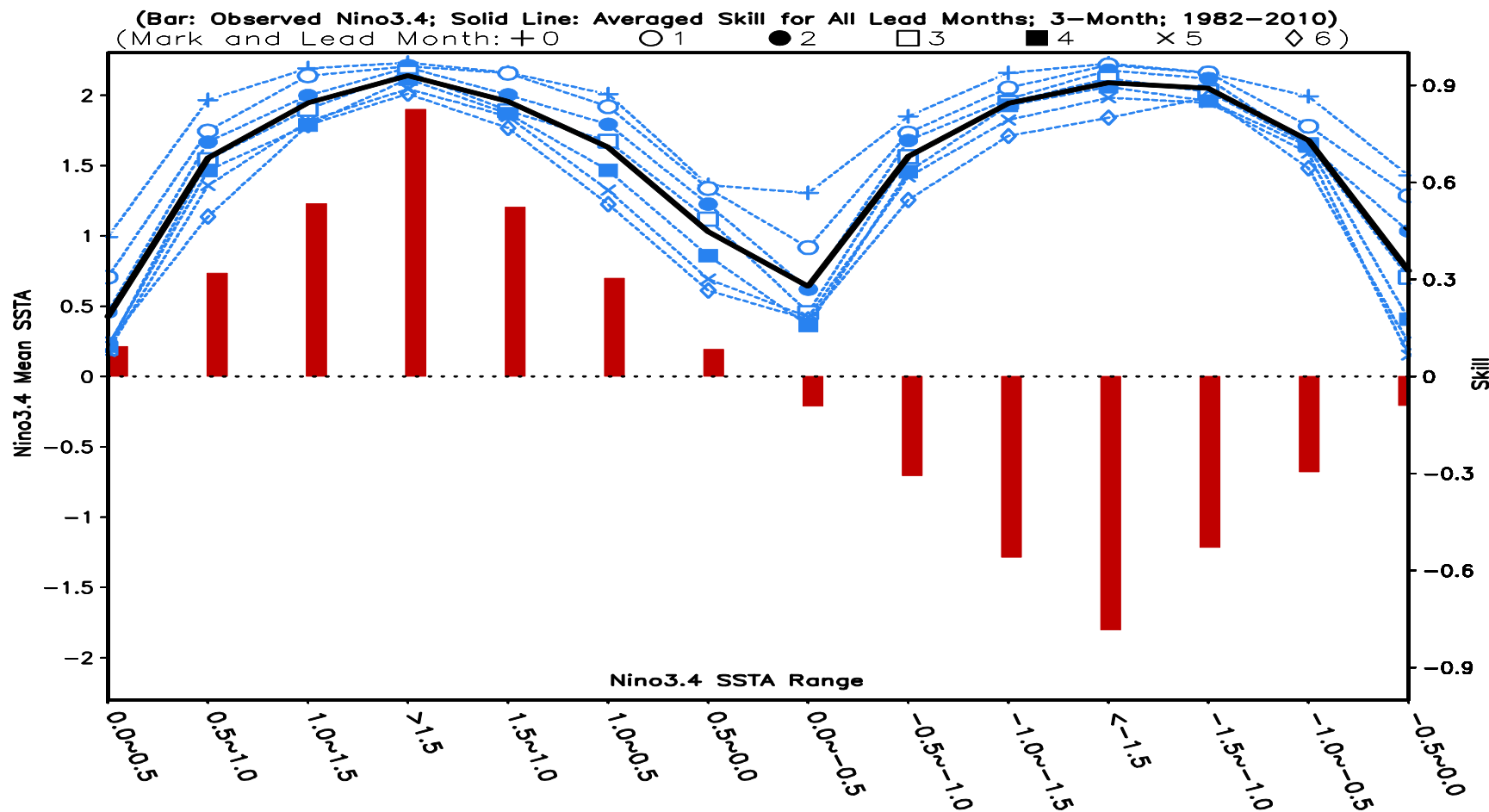
Dependence of prediction skills of CFSv2 predicted 3-month mean Niño3.4 index on lead time and Niño3.4 index amplitude based on OIv2 SSTA. Prediction skill is computed based on all forecasts in January 1982-December 2010. Red (gray) bars represent the skills when the initial amplitudes of OIv2 $|\text{Niño3.4 index}| > 0.5^\circ\text{C}$ ($|\text{Niño3.4 index}| \leq 0.5^\circ\text{C}$). The rightmost bar is the average for all 0-6 month leads.

14 ENSO phases classification based on OIv2 SSTA range and tendency. The numbers in the most right column show the % of number of month in each phase to total months in all phases.

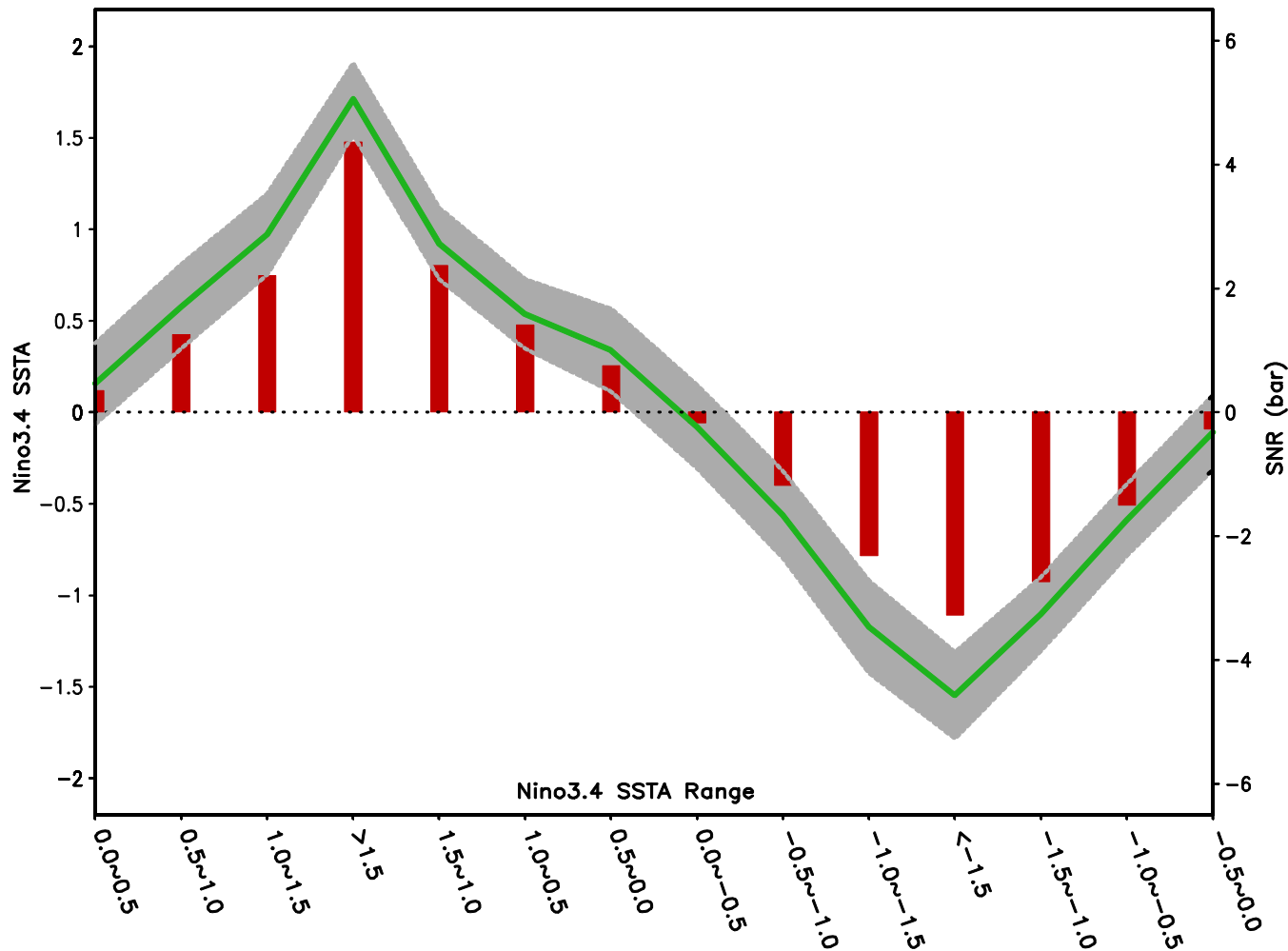
Phase	SSTA Range	SSTA Tendency	% of each phase
1	0.0°C ~ 0.5°C	Positive	12
2	0.5°C ~ 1.0°C	Positive	8
3	1.0°C ~ 1.5°C	Positive	4
4	> 1.5°C	Both positive and negative	7
5	1.5°C ~ 1.0°C	Negative	4
6	1.0°C ~ 0.5°C	Negative	7
7	0.5°C ~ 0.0°C	Negative	8
8	0.0°C ~ -0.5°C	Negative	8
9	-0.5°C ~ -1.0°C	Negative	9
10	-1.0°C ~ -1.5°C	Negative	5
11	< -1.5°C	Both positive and negative	4
12	-1.5°C ~ -1.0°C	Positive	4
13	-1.0°C ~ -0.5°C	Positive	10
14	-0.5°C ~ 0.0°C	Positive	10

Dependence of prediction skill on ENSO phase

(computed using same mean, but respective STDV in each phase)



Dependence of prediction skill of CFSv2 predicted 3-month mean Niño3.4 index on lead time and 14 ENSO phases classified based on OIv2 SSTA and its tendency (see Table 1 for details). Bars represent the Niño3.4 index based on OIv2 SSTA. Blue dashed lines with different marks are the prediction skill at different lead month and black solid line is the mean skill averaged all lead times. The amplitude of the Niño3.4 index is on the left y-axis while the prediction skill is on the right y-axis. The x-axis is the range of Niño3.4 index for different phases of ENSO. The analysis is based on all forecasts in January 1982-December 2010.



Noise (spread; shading) keeps almost constant during different phase of ENSO;

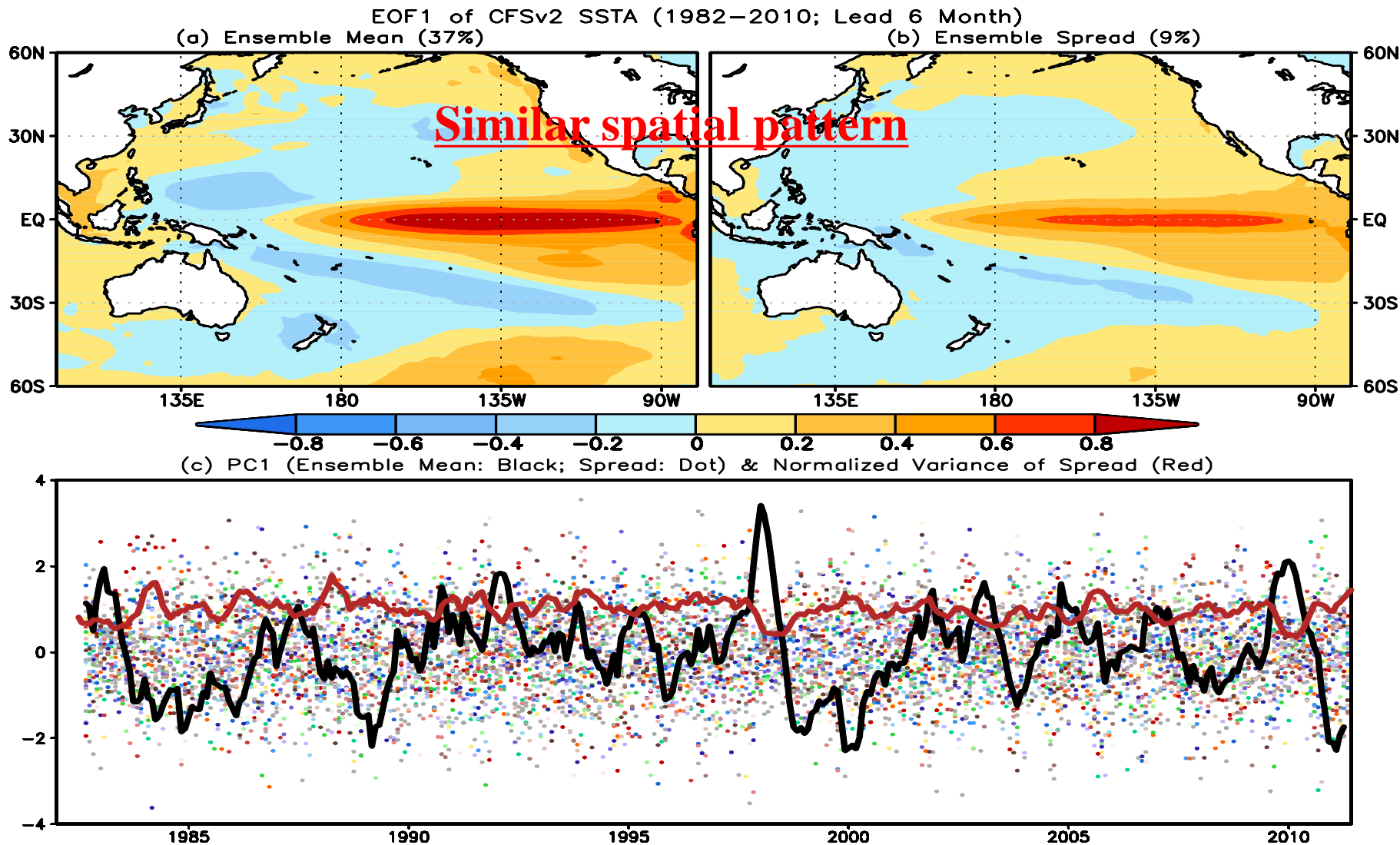
SNR (bar) almost solely depends on ensemble mean SSTA (signal, green line).

Dependence of ensemble mean (green line) and spread range superimposed on the forecast ensemble mean (shading) of CFSv2 predicted 3-month mean Niño3.4 index on 14 ENSO phases classified based on OIv2 SSTA and its tendency (see Table 1 for details). The spread range (shading) is referred to as one standard deviation of the spread. Both the ensemble mean and spread are for the average of 0-6 month lead hindcasts. Bars represent the corresponding SNR. The amplitude of the Niño3.4 index is on the left y-axis while the SNR is on the right y-axis. The x-axis is the range of Niño3.4 index for different phases of the ENSO cycle. The analysis is based on all forecasts in Jan1982 - Dec2010. 42

ENSO forecast skill varies with ENSO cycle
and is linked to SNR, which is determined
by SIGNAL, and NOISE is almost
temporally independent on SIGNAL

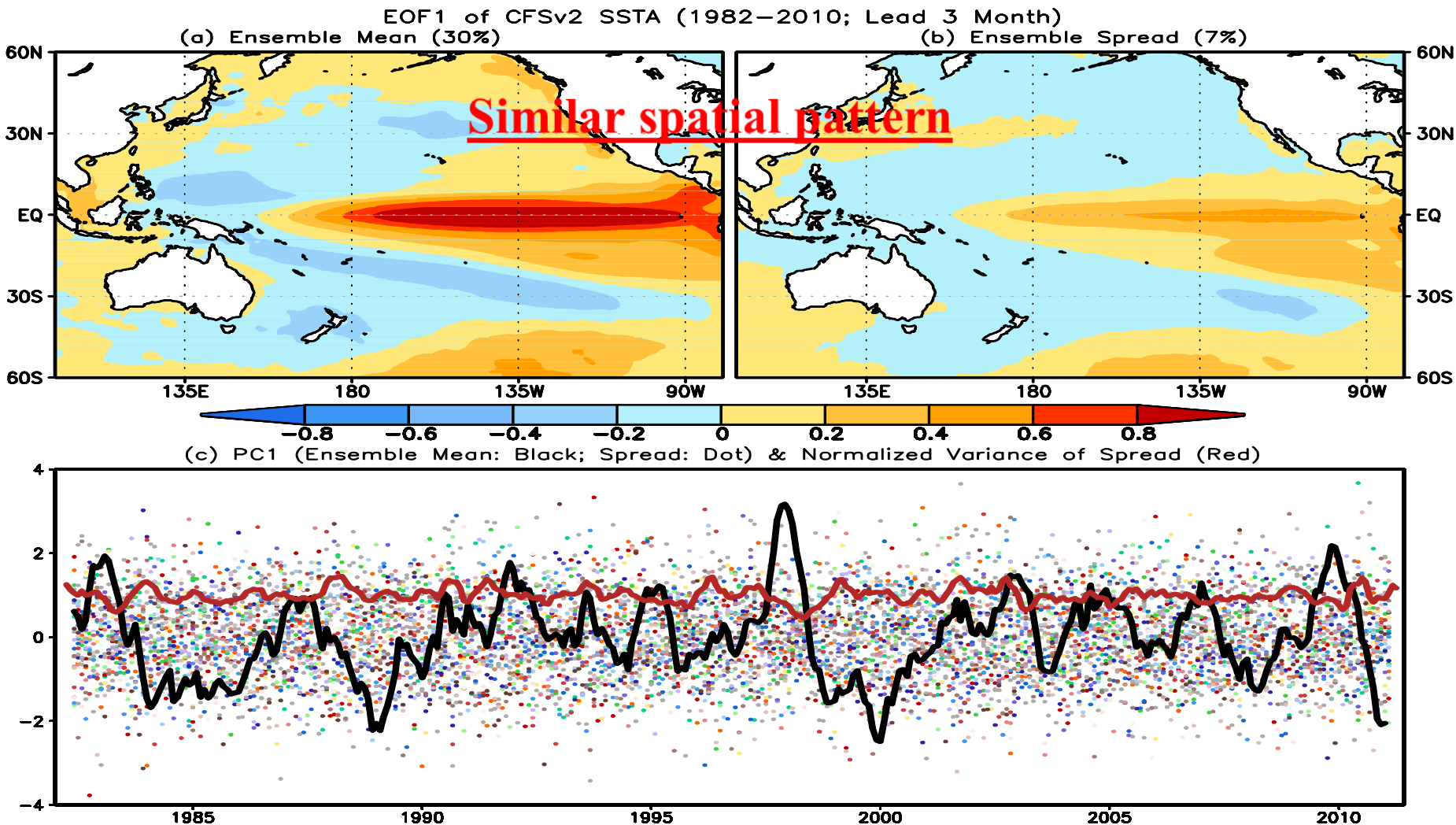
Are there any similarities for leading
pattern of Signal and Noise?

EOF1 of signal & noise at 6-mon lead



EOF1 of ensemble mean (a) and (b) spread, and (c) PC1 of ensemble mean (black curve) and spread (dots) for 6-month lead forecasts. The red curve is the variance of spread PC1 normalized by its corresponding climatological variance.

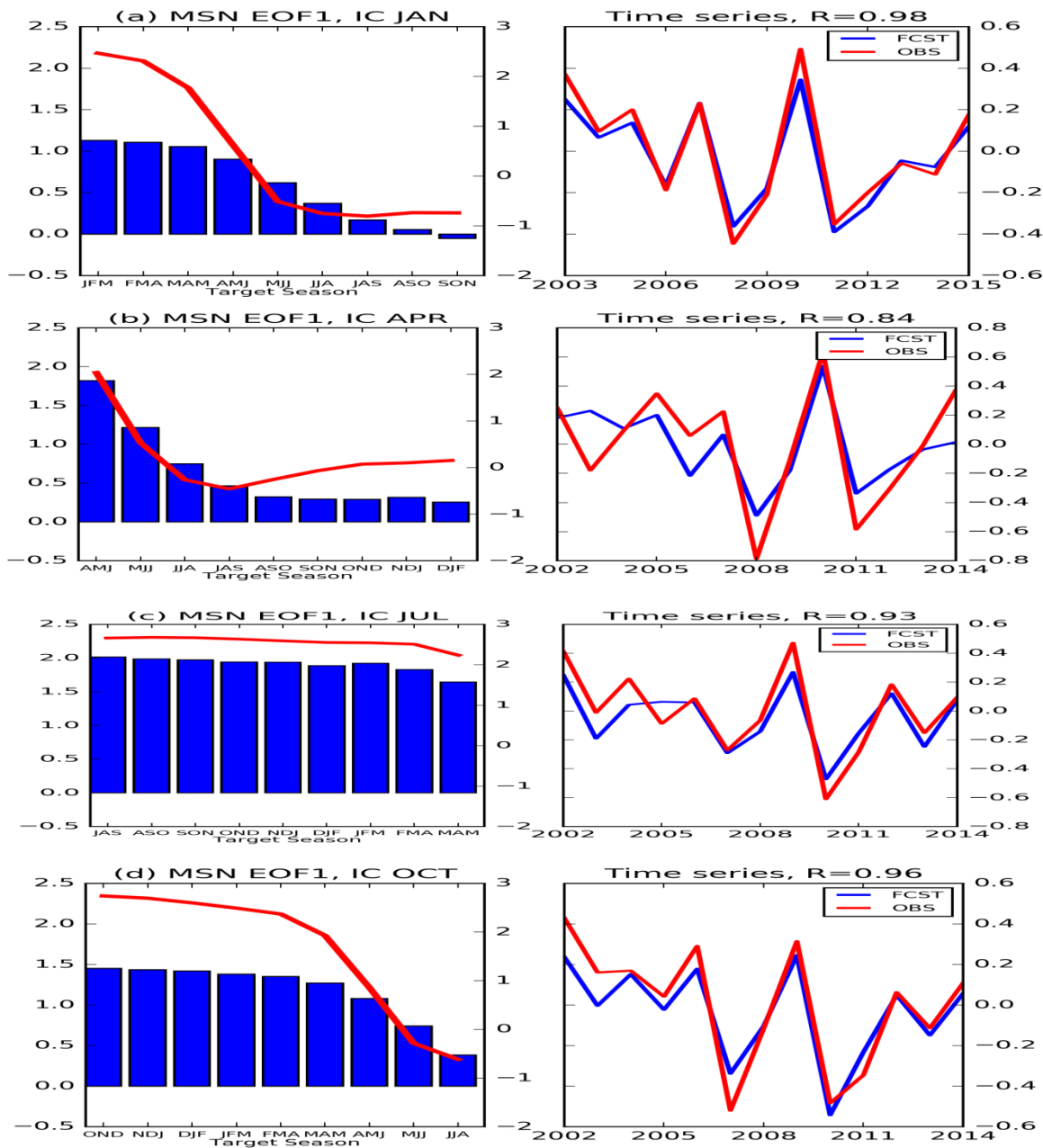
EOF1 of signal & noise at 3-mon lead



EOF1 of ensemble mean (a) and (b) spread, and (c) PC1 of ensemble mean (black curve) and spread (dots) for 3-month lead forecasts. The red curve is the variance of spread PC1 normalized by its corresponding climatological variance.

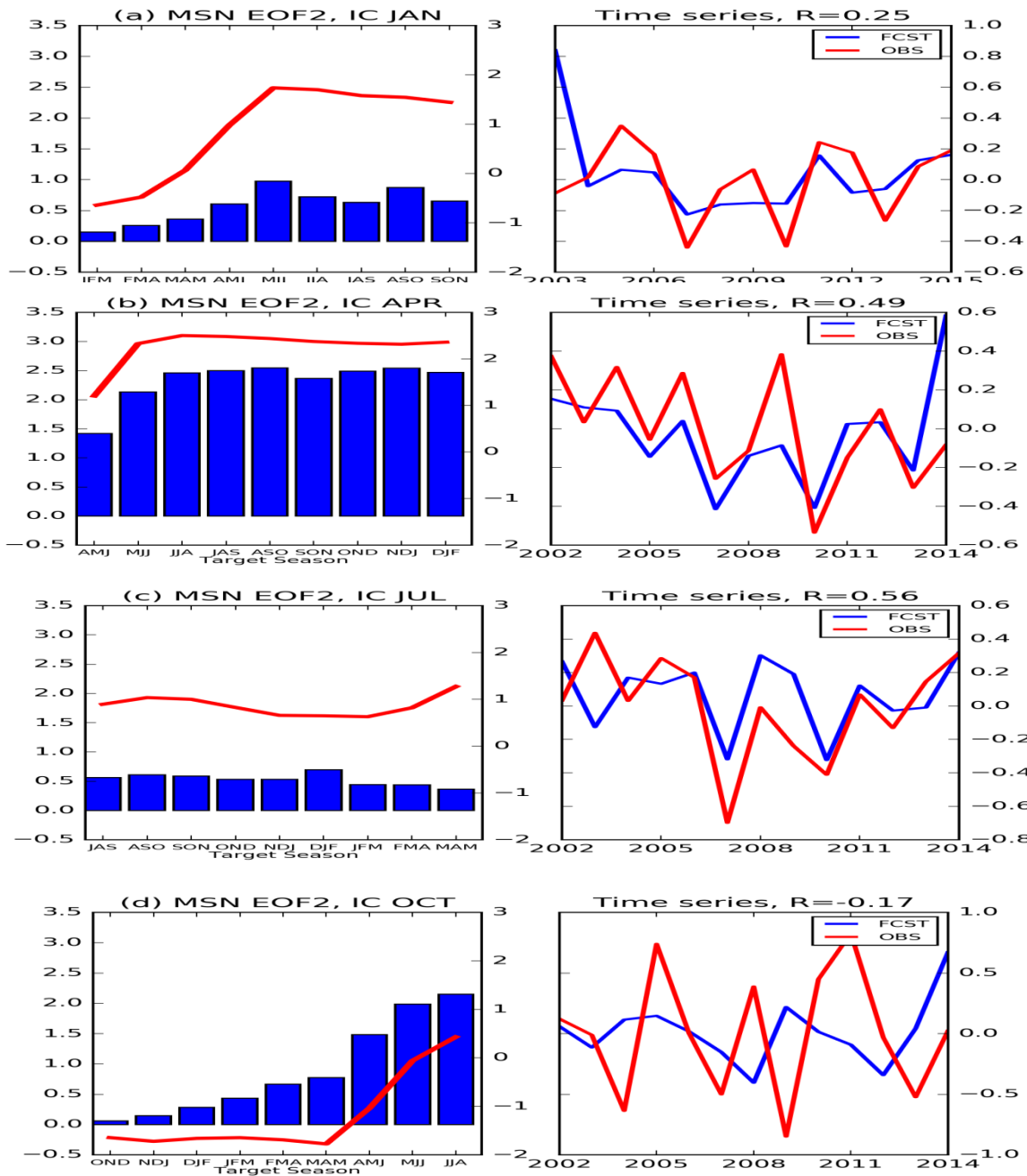
ENSO forecast skill varies with ENSO cycle

In fact, the predictability is not symmetric for development and decay phases of ENSO



The decay phase of ENSO is the most predictable evolution pattern among 20 IRI ENSO plume models.

MSN EOF1 and corresponding PC1 of the model forecasts for ICs in (a) Jan, (b) Apr, (c) Jul, and (d) Oct, respectively. In the left panel of each pair, the bars represent MSN EOF1, the red line is the composite of the observed evolution, which is defined as the differences between the mean of three maximum positive PC1 years minus the mean of maximum negative PC1 years in observation. The y-axis (on the right) in the bar-plot of each panel is for the scale of the observational composite (red curve). The red and blue lines in right panels of each pair are the corresponding PC1, which the projections of mean forecasts for all model means and observations onto the corresponding MSN EOF1, respectively.



MSN EOF2 sometime (IC=Jan, Oct) is associated with a development phase of ENSO with smaller explained variance.

The decay phase is more predictable than the development phase of ENSO.

MSN EOF2 and corresponding PC2 of the model forecasts for ICs in (a) Jan, (b) Apr, (c) Jul, and (d) Oct, respectively. In the left panel of each pair, the bars represent MSN EOF2, the red line is the composite of the observed evolution, which is defined as the differences between the mean of three maximum positive PC2 years minus the mean of maximum negative PC2 years in observation. The y-axis (on the right) in the bar-plot of each panel is for the scale of the observational composite (red curve). The red and blue lines in right panels of each pair are the corresponding PC2, which the projections of mean forecasts for all model means and observations onto the corresponding MSN EOF2, respectively.

- ENSO prediction skill varies with ENSO cycle: larger/smaller amplitude of Nino3.4 SSTA, higher/lower skill;
- Skill is linked to SNR, which is determined by signal and almost independent on noise;
- It is an inherent challenge to predict the development/transition phase of ENSO due to small SNR or signal;
- Noise and signal are temporally uncorrelated, but they have similar spatial distribution pattern;
- Asymmetry of predictability of ENSO: The decay phase is more predictable than the development phase of ENSO.

Acknowledgements

- Drs. Caihong Wen, Yan Xue, and Arun Kumar: reviewed PPT, and provide insight and constructive suggestions and comments
- Drs. Li Ren and Pingping Xie provided the BASS/CMORPH/CFSR EVAP package
- Dr. Emily Becker provided the NMME NINO3.4 plot
- Dr. Dan Collins provided the CPC ENSO consolidation plot

Backup Slides

Global Sea Surface Salinity (SSS)

Anomaly for February 2019

- **New Update:** The input satellite sea surface salinity of SMAP from NSAS/JPL was changed from Version 4.0 to Near Real Time product in August 2018.
- **Attention:** There is no SMAP SSS available in July 2018
- The large scale of negative SSS signal between equator and 20°N in the Pacific Ocean continues but such signal becomes weaker. The negative SSS signal appears along the equatorial Pacific Ocean, particularly nearby dateline in the west basin and nearby 105°W in the east basin. The SSS in the Bay of Bengal becomes saltier, especially in the west basin. The positive SSS signal in the majority of the N. Atlantic Ocean from equator to 40°N continues. Meanwhile, the negative SSS in the equatorial Atlantic is co-incident with increased precipitation.

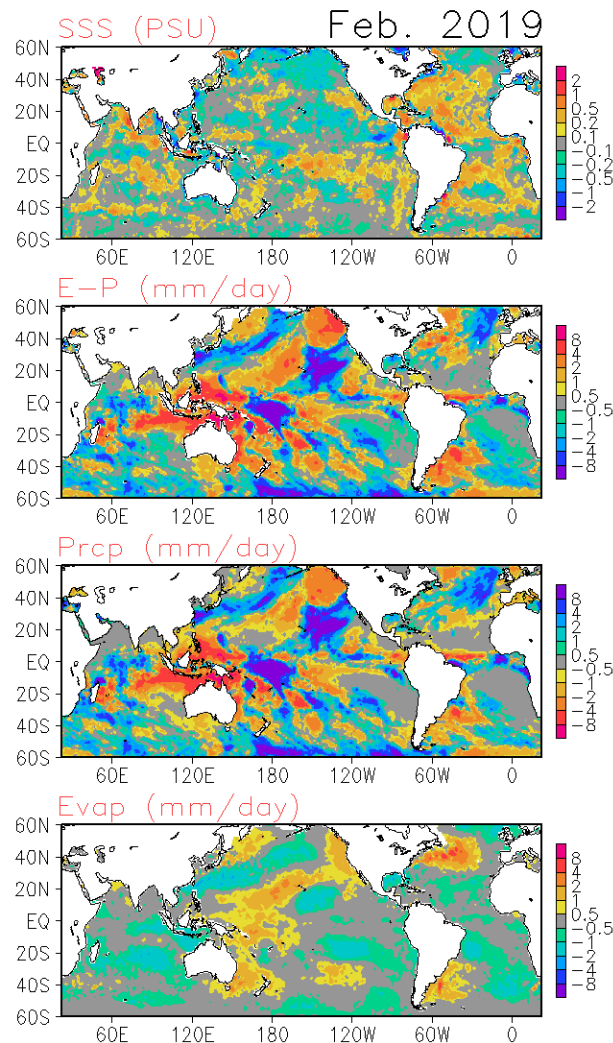
Data used

SSS : Blended Analysis of Surface Salinity (BASS) V0.Z
(a CPC-NESDIS/NODC-NESDIS/STAR joint effort)
(Xie et al. 2014)

<ftp.cpc.ncep.noaa.gov/precip/BASS>

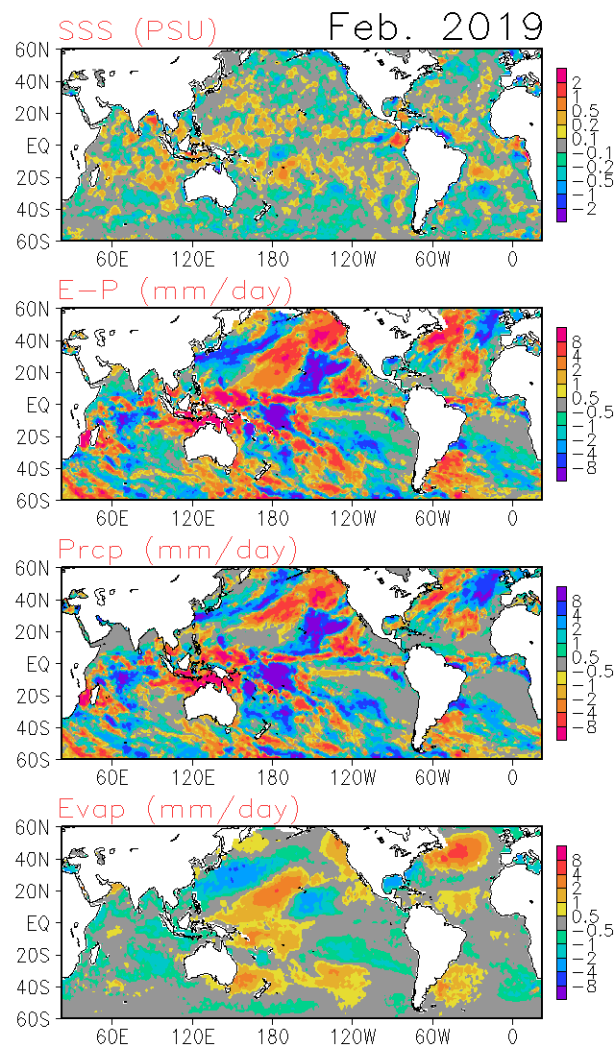
Precipitation: CMORPH adjusted satellite precipitation estimates

Evaporation: Adjusted CFS Reanalysis



Global Sea Surface Salinity (SSS) Tendency for February 2019

Compared with last month, the SSS increased between equator and 20°N in the Pacific Ocean, especially in the west basin, which is coincident with reduced precipitation. The SSS decreased along the Equatorial Pacific ocean. The SSS decreased in most of the areas in the southern Ocean (south of 40°S), which is likely caused by oceanic advection and/or entrainments.

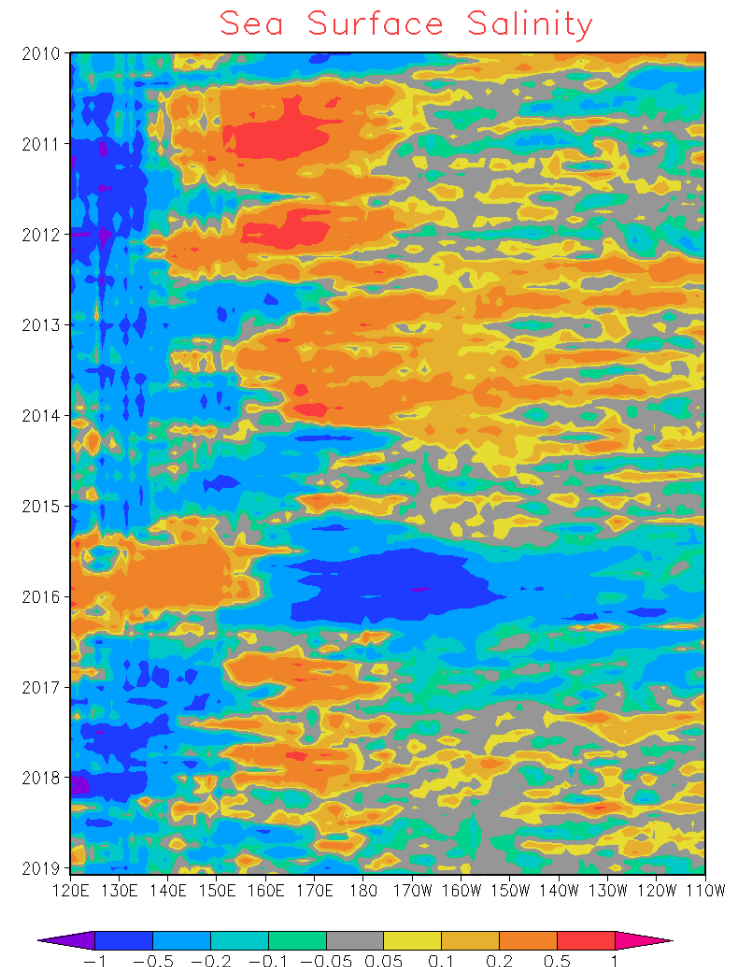


Global Sea Surface Salinity (SSS)

Anomaly Evolution over Equatorial Pacific from Monthly SSS

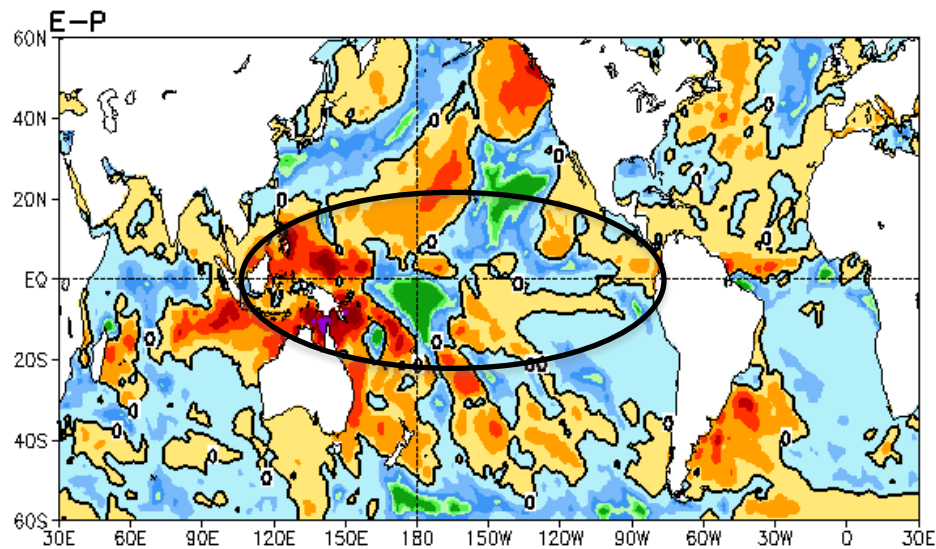
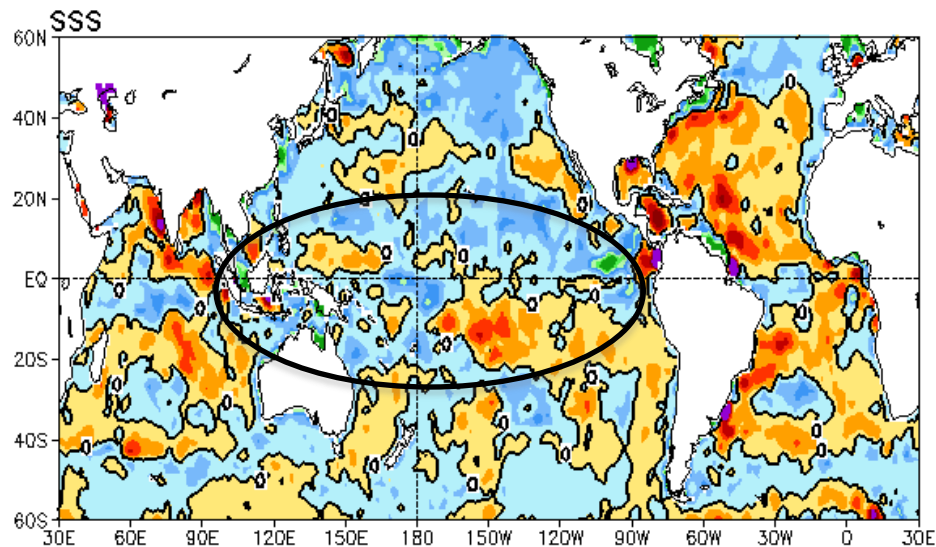
NOTE: Since June 2015, the BASS SSS is from in situ, SMOS and SMAP; before June 2015, The BASS SSS is from in situ, SMOS and Aquarius.

- Hovemoller diagram for equatorial SSS anomaly (**5°S-5°N**);
- In the equatorial Pacific Ocean, the negative SSS signal continues from 120°E to 180°E, the negative SSS signal appears east of 150°W and it is stronger east of 120°W.



Monitoring SSS and Freshwater Flux Variability

FEB 2019 SSS Anomaly (PSU) & E-P Anomaly (mm/day)



- **Blended Analysis of Surface Salinity (BASS): In Situ, SMOS, Aquarius and SMAP**

- **2010-2018, Monthly and Pentad**
- **CPC/NODC/NESDIS joint effort (Xie et al. 2014)**

<ftp.cpc.ncep.noaa.gov/precip/BASS>

- **Precipitation: CMORPH**

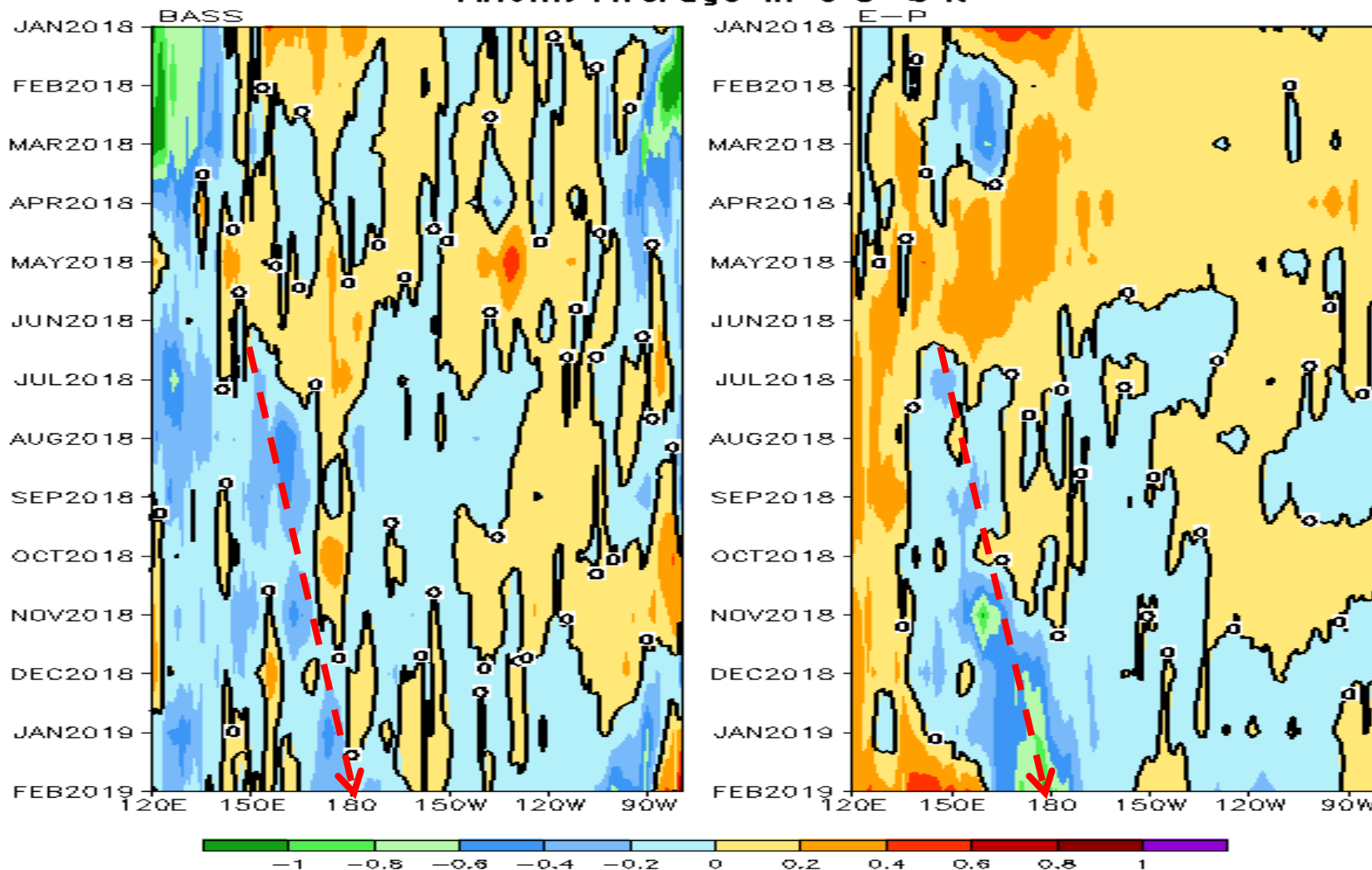
- **Evaporation: CFSR adjusted to OAFlux**

- **SSS and E-P anom. in the tropical Pacific were associated the El Nino conditions.**

SSS Anom

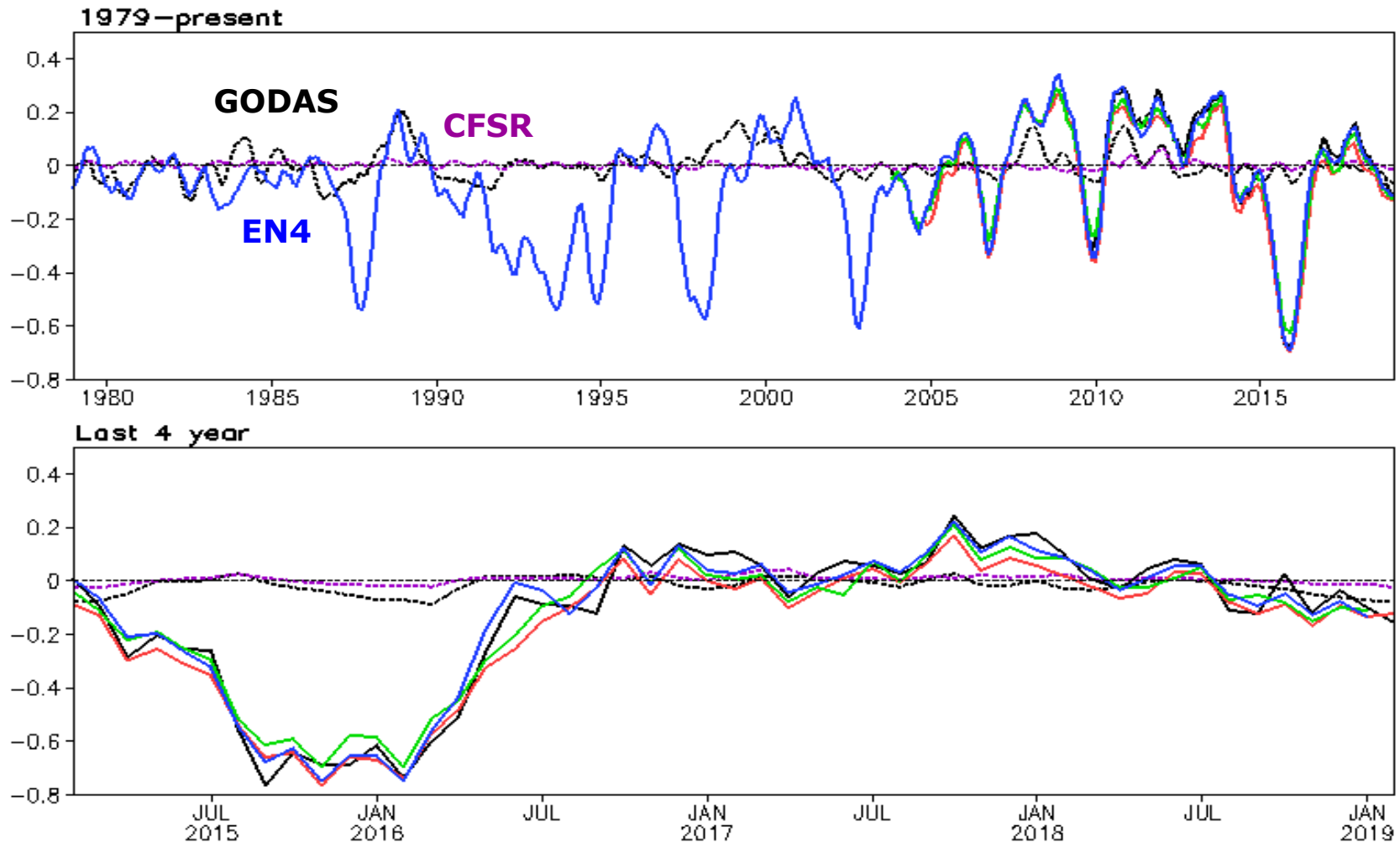
E-P Anom

Anom. Average in 5°S–5°N



- Negative SSS anom. extended gradually eastward since Jul 2018, consistent with the eastward propagation of E-P anom..
- The low frequency signal of SSS and E-P anom. were associated with the 2018/19 El Nino.

SSS Anom. in [160E-160W, 5S-5N] (PSU), Levitus Clim
GODAS (dash black), CFSR (dash purple), BASS (solid black)
IPRC (red), SCRIPPS (green), EN4.2.1 (blue)

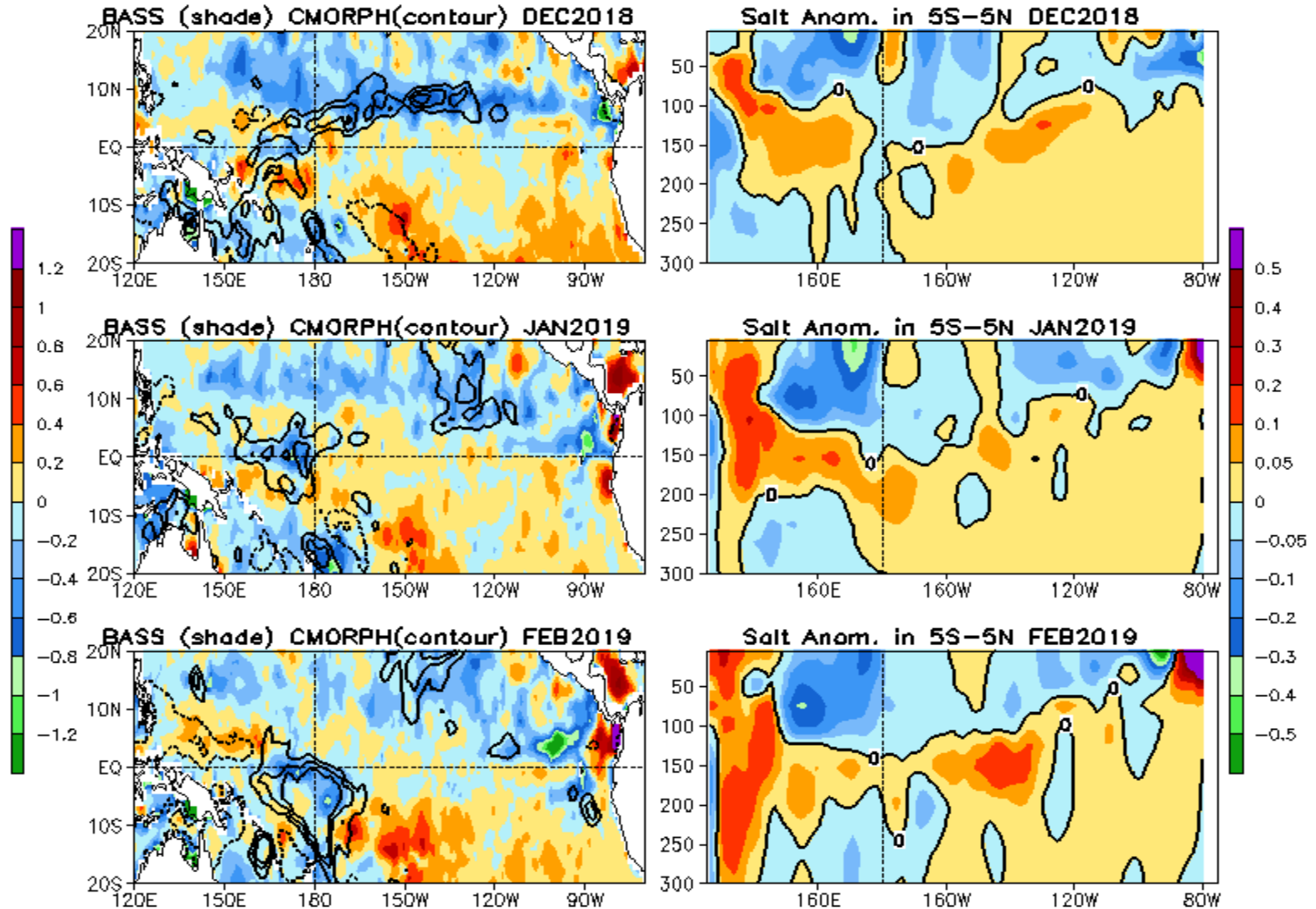


- SSS anom. in [160E-160W, 5S-5N] is consistent among the BASS and in situ data-based objective analyses (EN4.2.1, IPRC and Scripps Argo).

- **GODAS severely underestimates SSS variability due to assimilation of synthetic salinity.**

**SSS Anom. (shade)
Prec. Anom. (contour)**

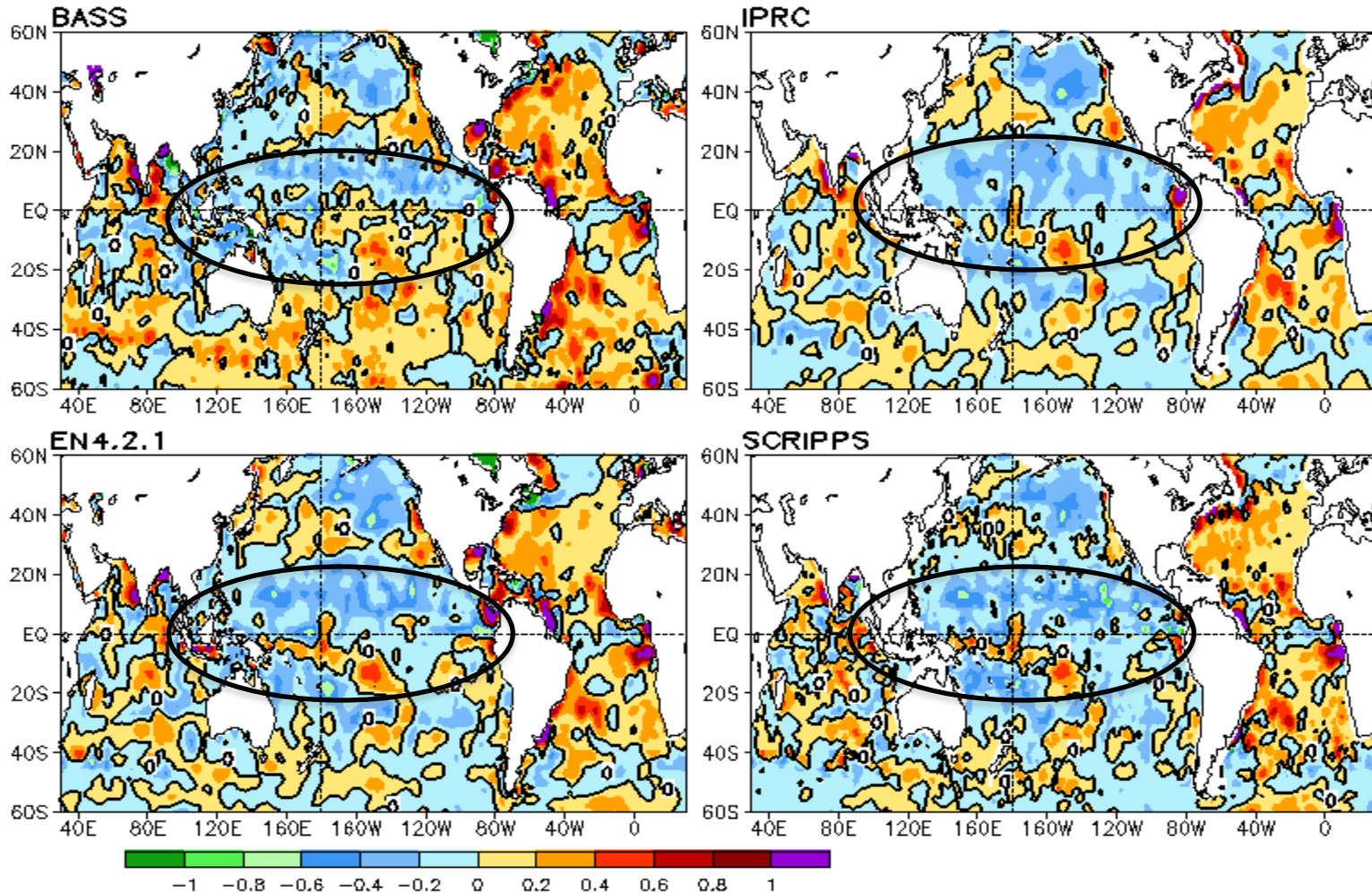
**Salt Anom. in 5S-5N
(Mean of EN4, IPRC and Scripps)**



- Negative salinity anom. presented in upper 100m in 150E-180E and 140W-90W in the last three months.

Uncertainty in SSS Anomaly

JAN 2019 SSS Anomaly (PSU), Levitus Clim



IPRC Argo (2005-present, real-time): <http://apdrc.soest.hawaii.edu/projects/argo/>
SCRIPPS Argo (2004-present, one-month delay): http://sio-argo.ucsd.edu/RG_Climatology.html
EN4.2.1 (1900-present, one-month delay): <https://www.metoffice.gov.uk/hadobs/en4/download-en4-2-1.html>

Data Sources and References

(climatology is for 1981-2010)

- **Weekly Optimal Interpolation SST (OI SST) version 2 (Reynolds et al. 2002)**
- **Extended Reconstructed Sea Surface Temperature (ERSST) v5 (Huang et al. 2017)**
- **Blended Analysis of Surface Salinity (BASS) (Xie et al. 2014)**
- **CMORPH precipitation (Xie et al. 2017)**
- **CFSR evaporation adjusted to OAFlux (Xie and Ren 2018)**
- **NCEP CDAS winds, surface radiation and heat fluxes (Kalnay et al. 1996)**
- **NESDIS Outgoing Long-wave Radiation**
- **NCEP's Global Ocean Data Assimilation System temperature, heat content, currents (Behringer and Xue 2004)**
- **Aviso altimetry sea surface height from CMEMS**
- **Ocean Surface Current Analyses – Realtime (OSCAR)**
- **In situ data objective analyses (IPRC, Scripps, EN4.2.1, PMEL TAO)**
- **Operational ocean reanalyses from Real-time Ocean Reanalysis Intercomparison Project**

http://www.cpc.ncep.noaa.gov/products/GODAS/multiora_body.html

http://www.cpc.ncep.noaa.gov/products/GODAS/multiora93_body.html

Tropical Pacific: SST Anom., SST Anom. Tend., OLR, Sfc Rad, Sfc Flx, 925-mb & 200-mb Winds

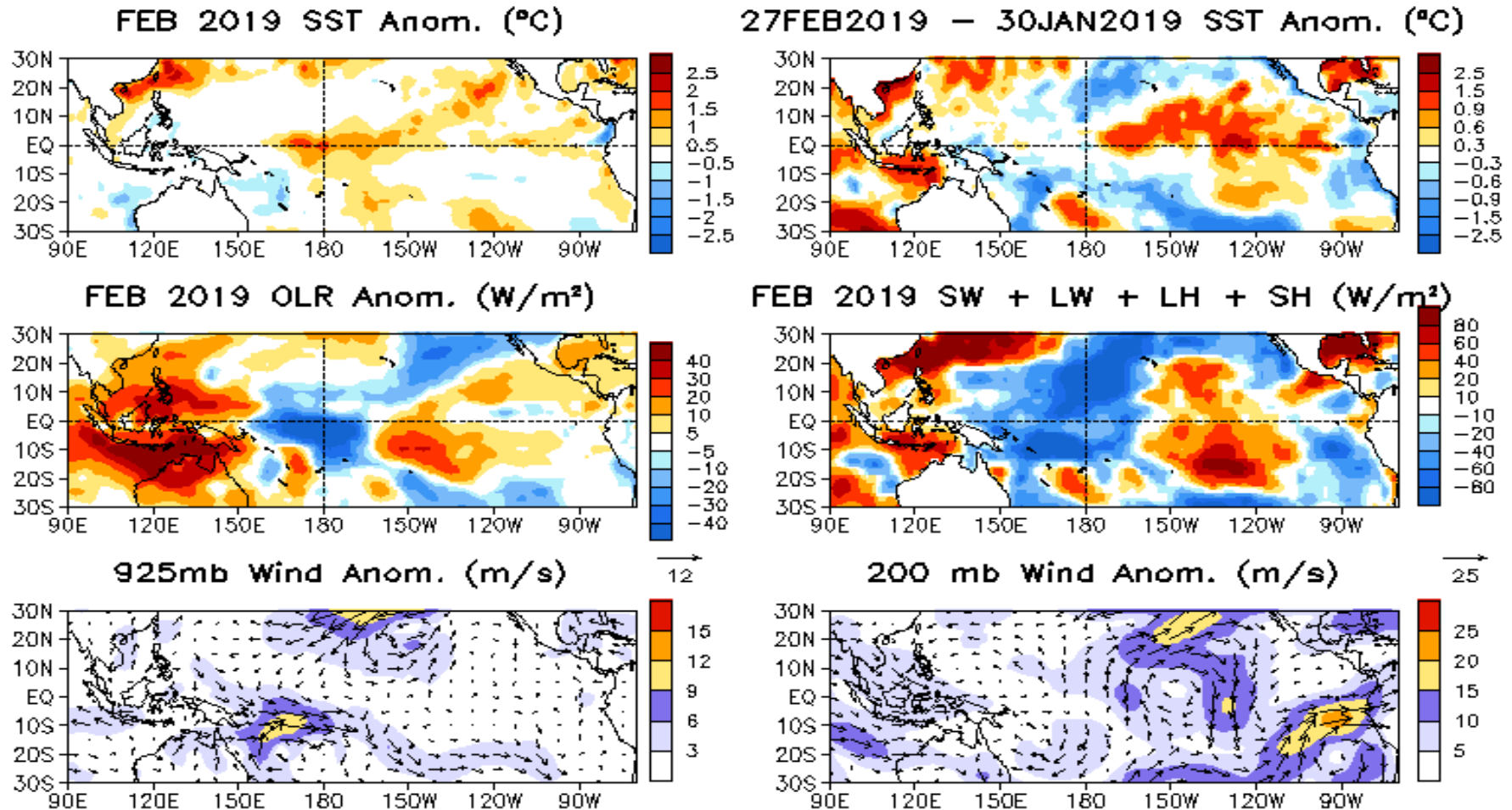
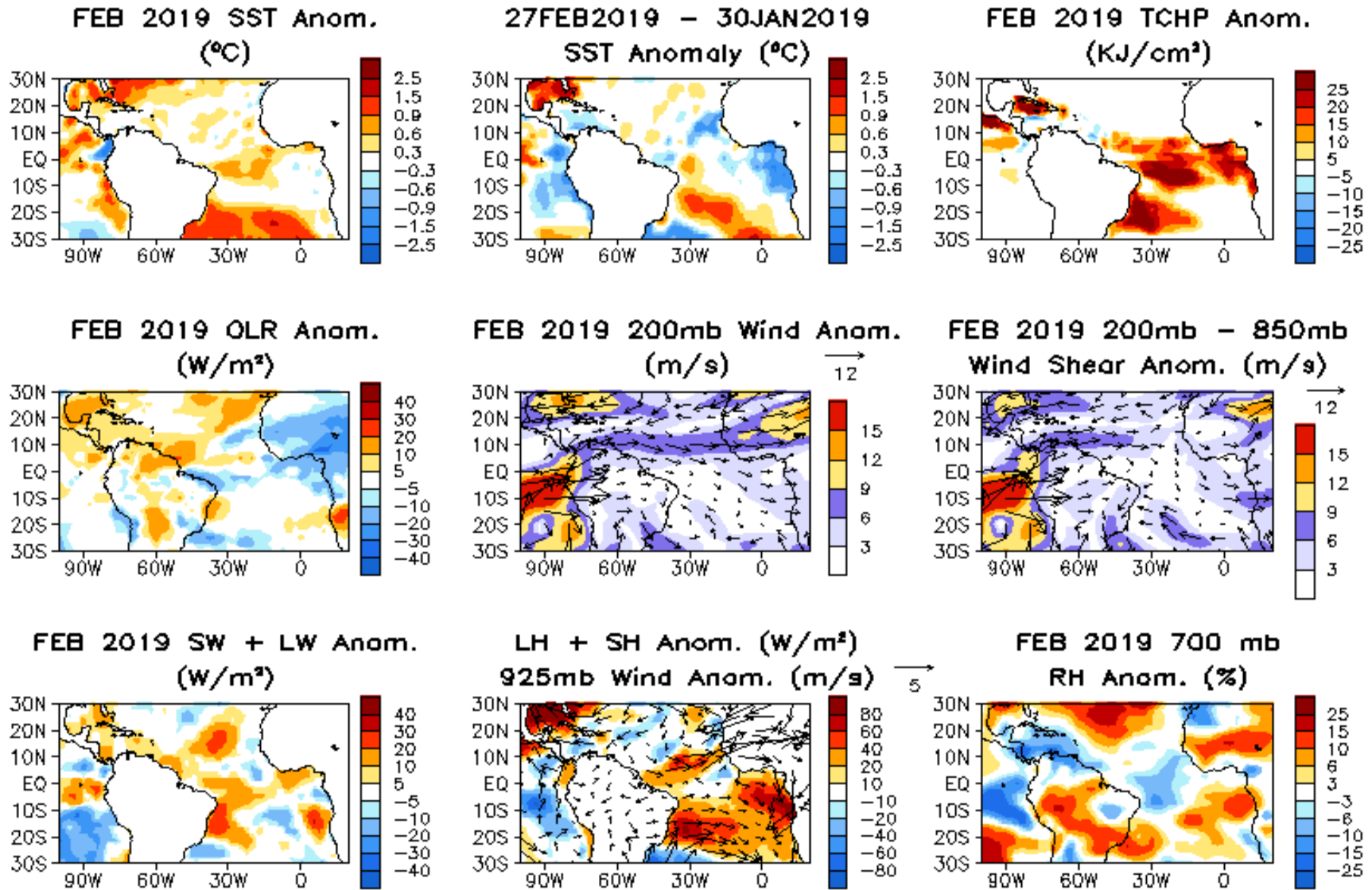


Fig. P2. Sea surface temperature (SST) anomalies (top-left), anomaly tendency (top-right), Outgoing Long-wave Radiation (OLR) anomalies (middle-left), sum of net surface short- and long-wave radiation, latent and sensible heat flux anomalies (middle-right), 925-mb wind anomaly vector and its amplitude (bottom-left), 200-mb wind anomaly vector and its amplitude (bottom-right). SST are derived from the NCEP OI SST analysis, OLR from the NOAA 18 AVHRR IR window channel measurements by NESDIS, winds and surface radiation and heat fluxes from the NCEP CDAS. Anomalies are departures from the 1981-2010 base period means.

Tropical Atlantic:



North Atlantic: SST Anom., SST Anom. Tend., OLR, SLP, Sfc Rad, Sfc Flx

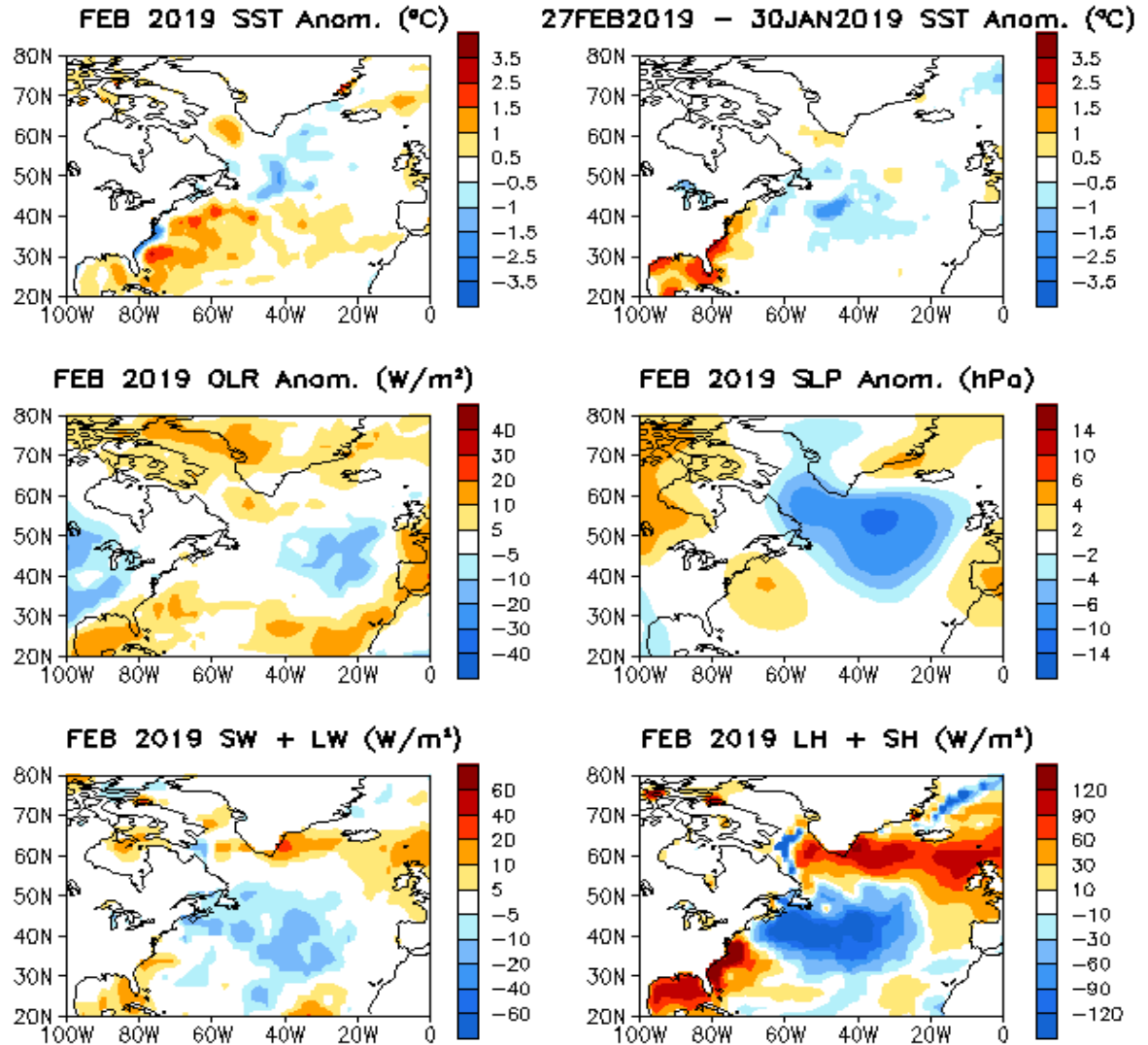


Fig. NA1. Sea surface temperature (SST) anomalies (top-left), anomaly tendency (top-right), Outgoing Long-wave Radiation (OLR) anomalies (middle-left), sea surface pressure anomalies (middle-right), sum of net surface short- and long-wave radiation anomalies (bottom-left), sum of latent and sensible heat flux anomalies (bottom-right). SST are derived from the NCEP OI SST analysis, OLR from the NOAA 18 AVHRR IR window channel measurements by NESDIS, sea surface pressure and surface radiation and heat fluxes from the NCEP CDAS. Anomalies are departures from the 1981-2010 base period means.

Data Sources and References

- **Optimal Interpolation SST (OI SST) version 2 (Reynolds et al. 2002)**
- **NCEP CDAS winds, surface radiation and heat fluxes**
- **NESDIS Outgoing Long-wave Radiation**
- **NDBC TAO data (<http://tao.ndbc.noaa.gov>)**
- **PMEL TAO equatorial temperature analysis**
- **NCEP's Global Ocean Data Assimilation System temperature, heat content, currents (Behringer and Xue 2004)**
- **Aviso Altimetry Sea Surface Height**
- **Ocean Surface Current Analyses – Realtime (OSCAR)**

Please send your comments and suggestions to Yan.Xue@noaa.gov. Thanks!